

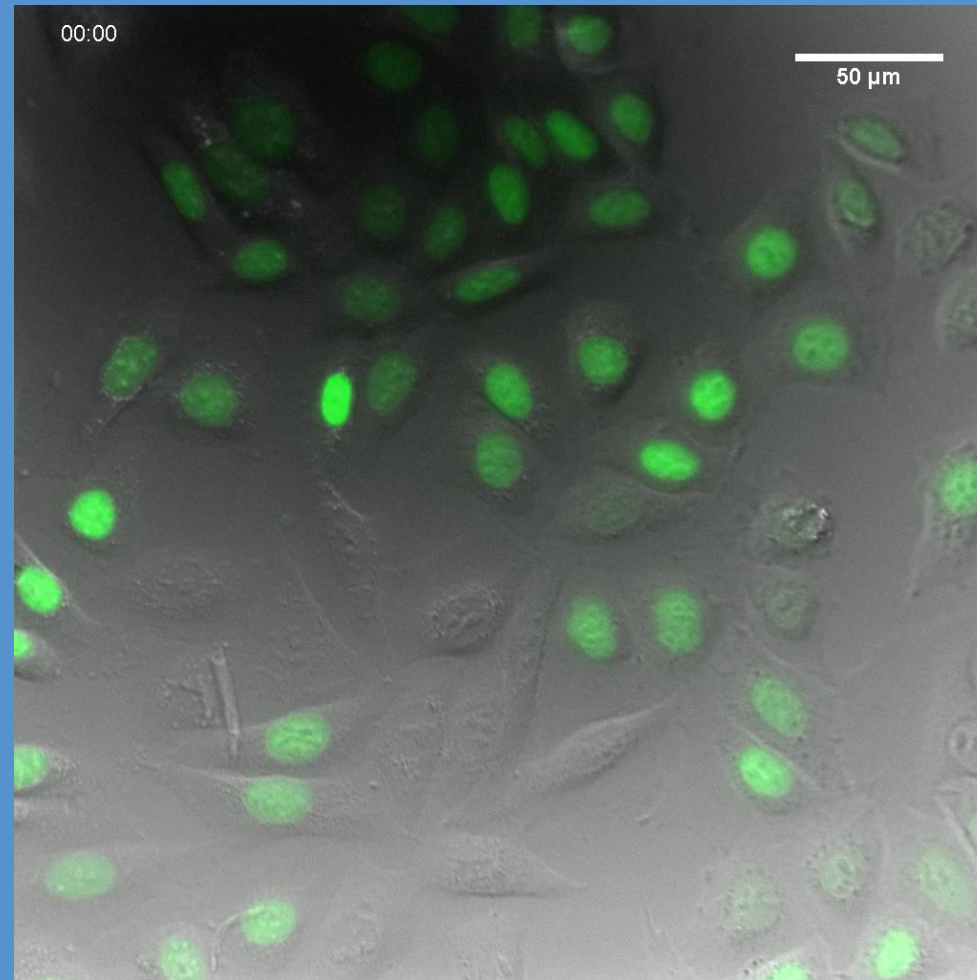


ONBI January, 2015

VIABILITY COMPARISON OF MICROSCOPE  
TECHNIQUES

Dr. B. Christoffer Lagerholm  
Wolfson Imaging Centre Oxford  
Facility Manager

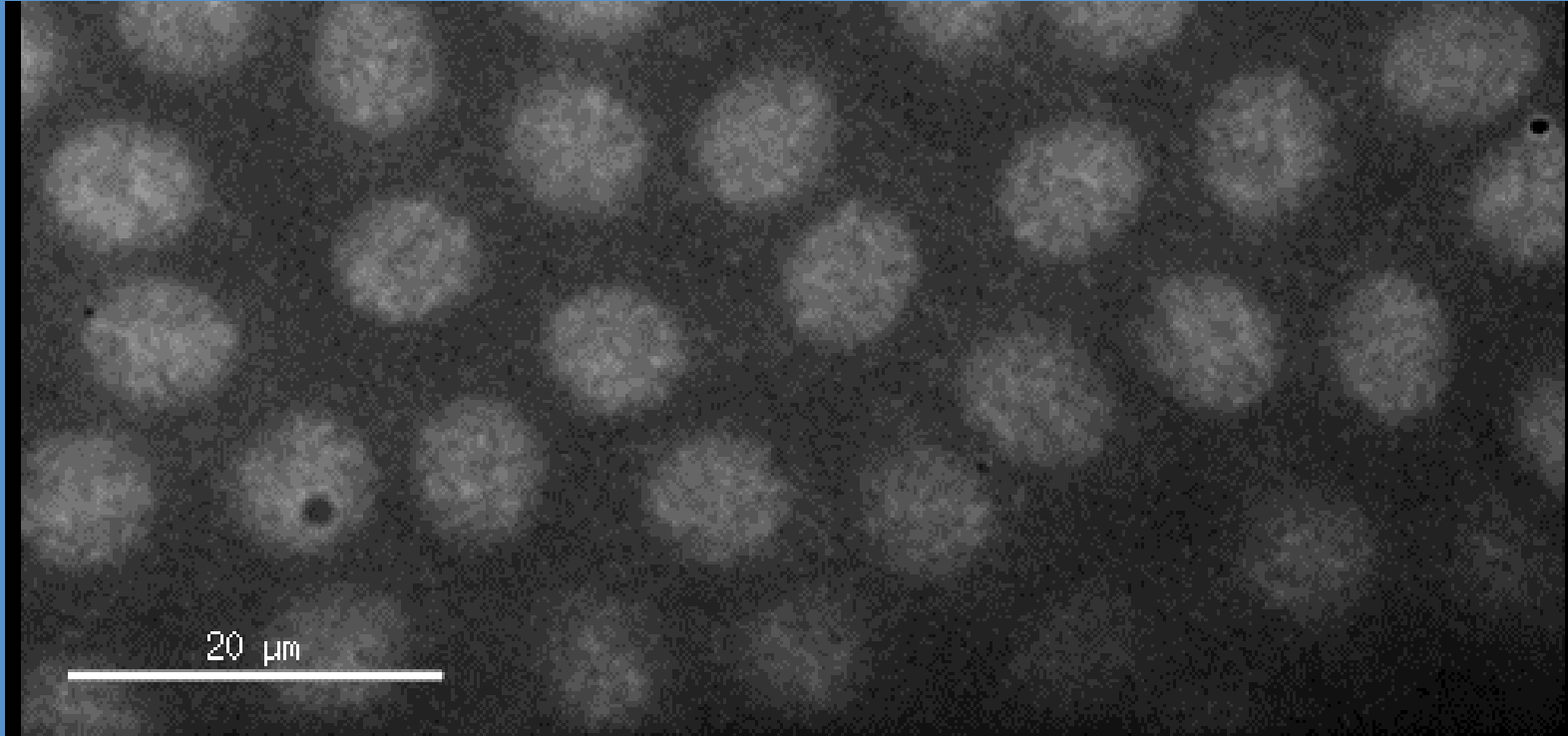
## Application Example: Long-term non-invasive in vitro imaging



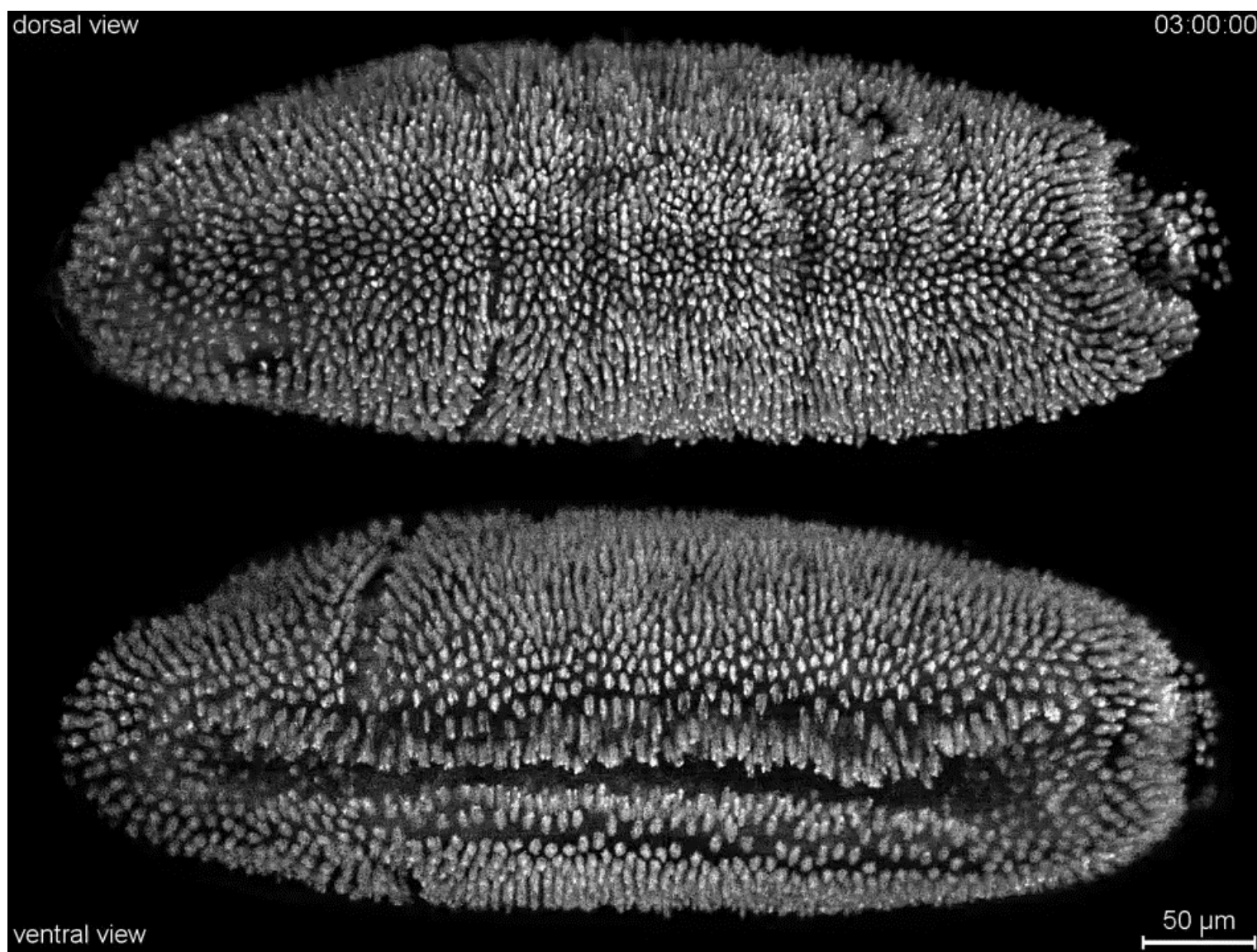
Live HeLa cell expressing Histone 2B-Green fluorescent protein (H2B-GFP) that was imaged at 10 min interval for  $\sim 24\text{h}$ .

# Application Example: Non-invasive in vivo imaging in Drosophila Embryos

Richard Parton, Dept. of Biochemistry; Veronica Buckle & Jill Brown, MHU WIMM

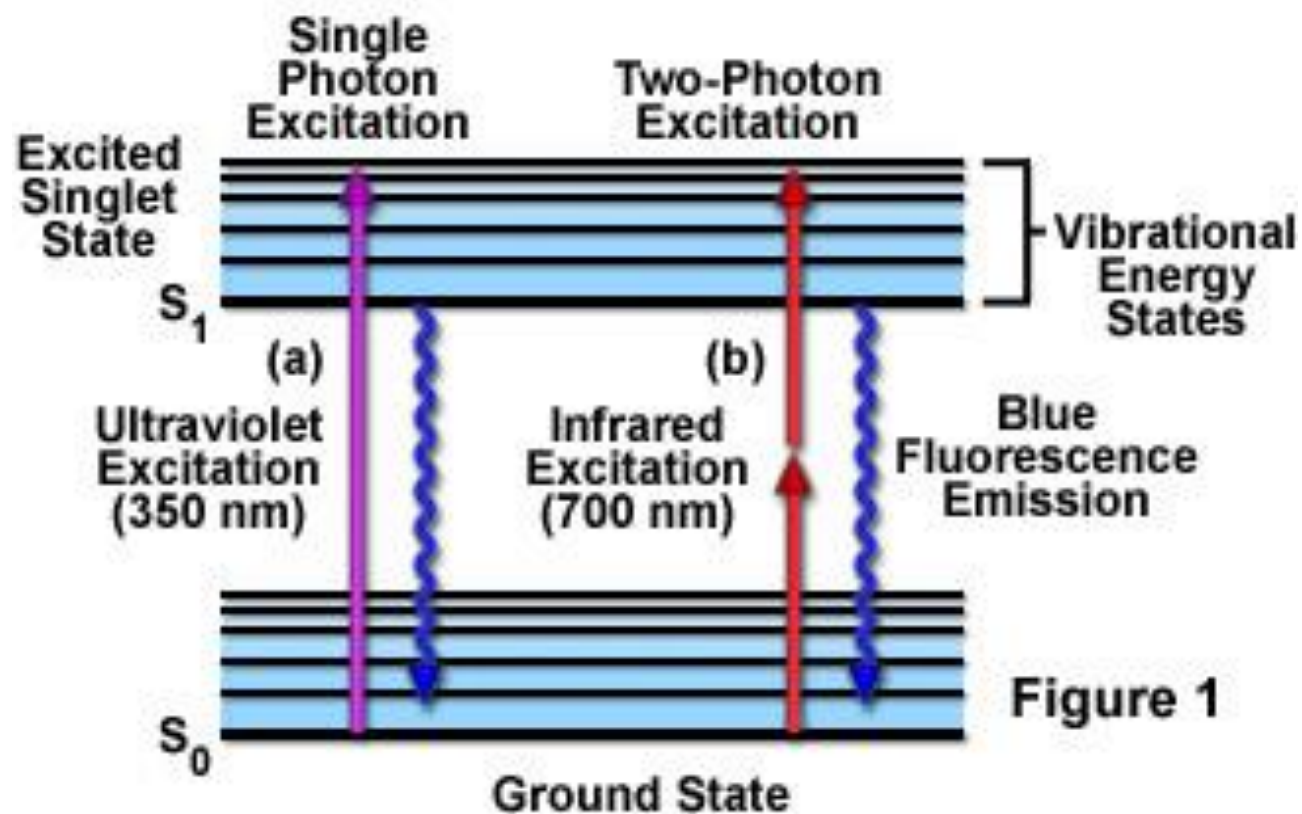


His2A-GFP



Simultaneous multiview imaging of *Drosophila* embryonic development (*His2Av-GFP<sup>S65T</sup>* transgenic stock). The embryo was recorded at 30-second intervals over a period of 17 hours, using an image acquisition period of 15 seconds per time point. The data set consists of 1,066,520 high-resolution images (11 terabytes). The video shows separate maximum-intensity projections of the first and second halves of the fused and background-corrected three-dimensional image stacks, providing dorsal and ventral views of the developing embryo. To reduce the file size of this video, frames were down-sampled by a factor of 2. Imaging framework: One-photon SiMView. Detection objectives: 2× Nikon CFI75 LWD 16×/0.80 W. Cameras: 2× Andor Neo sCMOS. Technical note: The occurrence of subtle stripe patterns arises from column gain variability in first-generation sCMOS cameras, such as the Andor Neo cameras used in this recording.

## Two-Photon Jablonski Energy Diagram

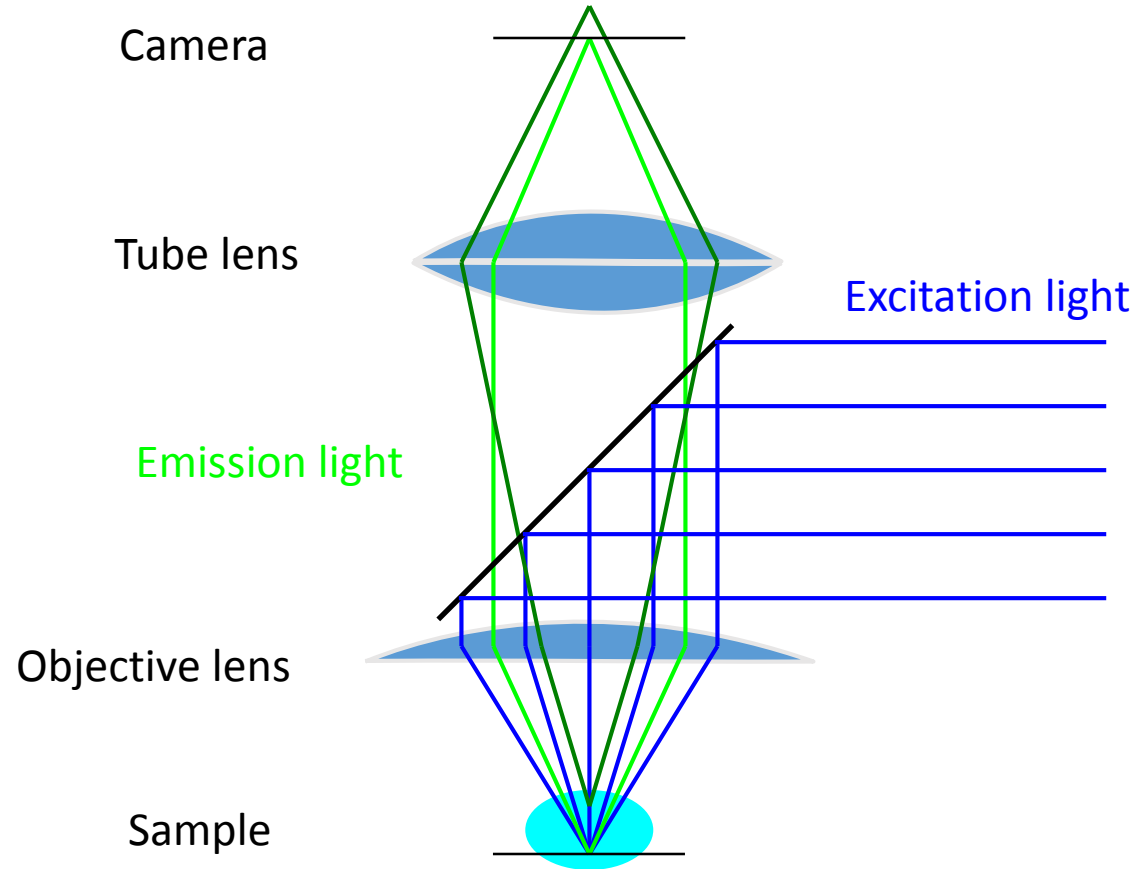


## DeltaVision Elite–Live Cell Imaging System



- The DeltaVision Elite is a conventional wide-field fluorescence microscope that has been optimized for: 1) high-sensitivity imaging in 3D, and 2) long-term time-lapse imaging of live cells at 37C and 5% CO<sub>2</sub>.
- This system is equipped with fluorescence filters for imaging e.g. DAPI, CFP, GFP, YFP, RFP, mCherry, and CY5.

# Wide-field Microscopy



Problem – fluorescence is emitted along entire illuminated cone, not just at focus

## Zeiss 780 Upright Confocal Microscope



- This Zeiss 780 Upright Confocal is a hybrid conventional laser-scanning confocal and multi-photon confocal microscope that has been optimized for high-sensitivity multi-color 3D imaging in thick specimens ( $t < 500-1000 \mu\text{m}$ )
- This system is equipped with conventional lasers (405, 458, 488, 514, 543, 594, and 633 nm), a tuneable (690-1040 nm) MAI TAI DeepSee laser for multi-photon excitation, and detectors for imaging in the visible spectrum ( $400 < \lambda < 700 \text{ nm}$ ).

# The confocal vs Two-photon microscope

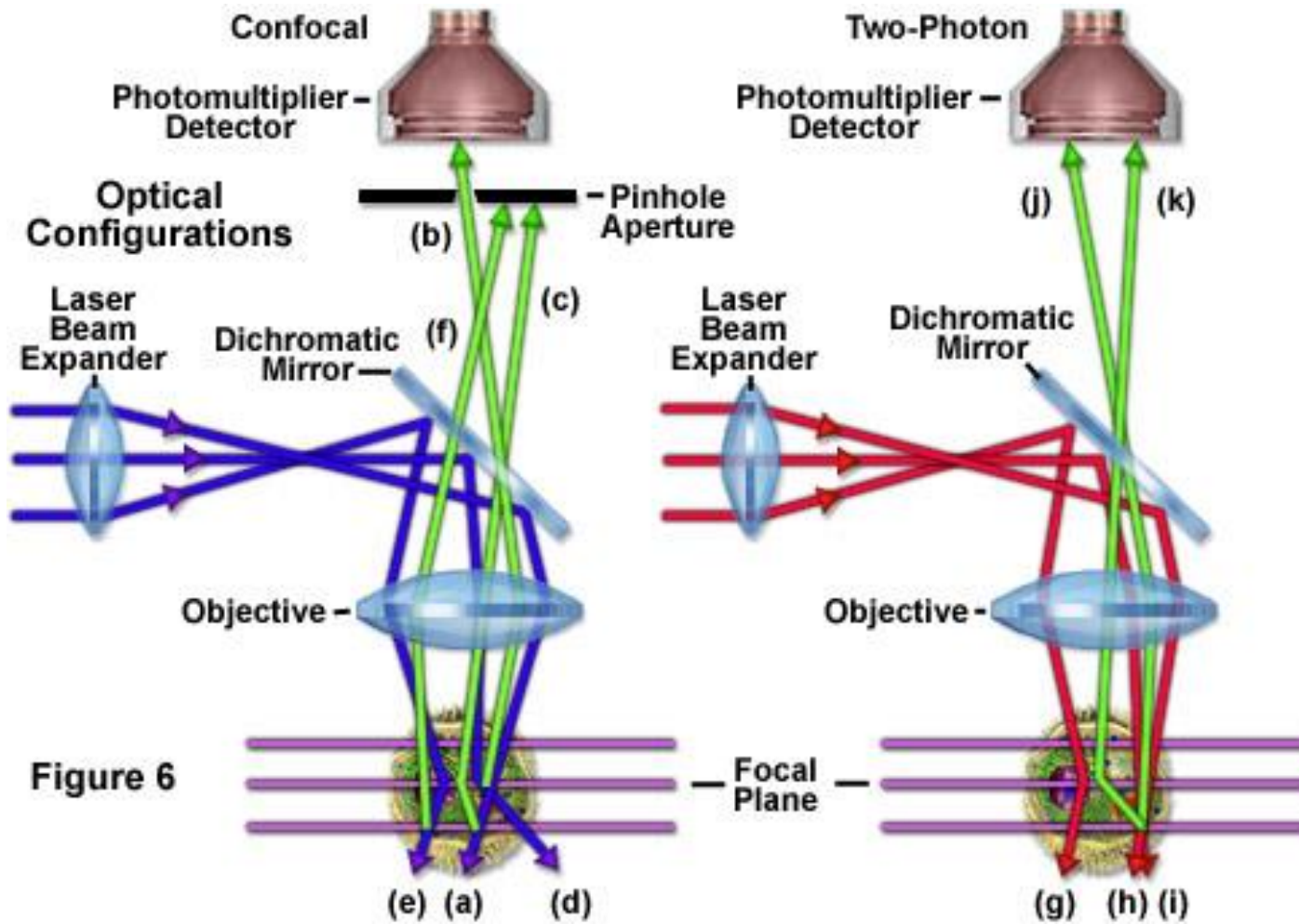
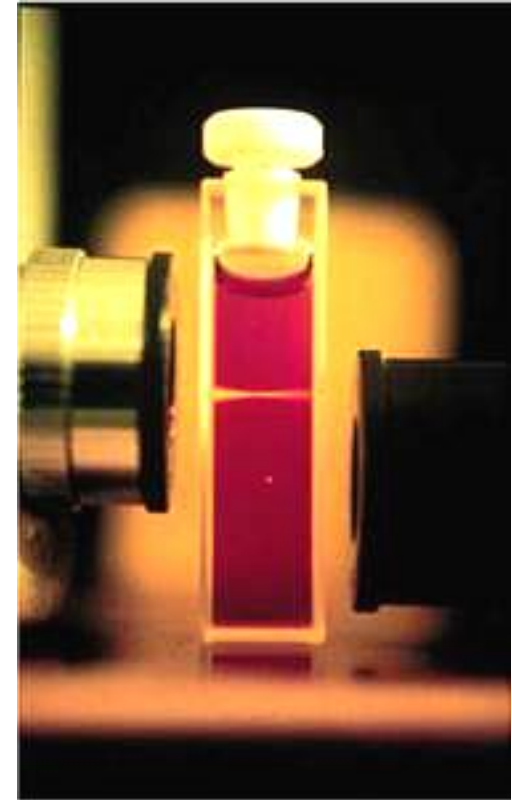
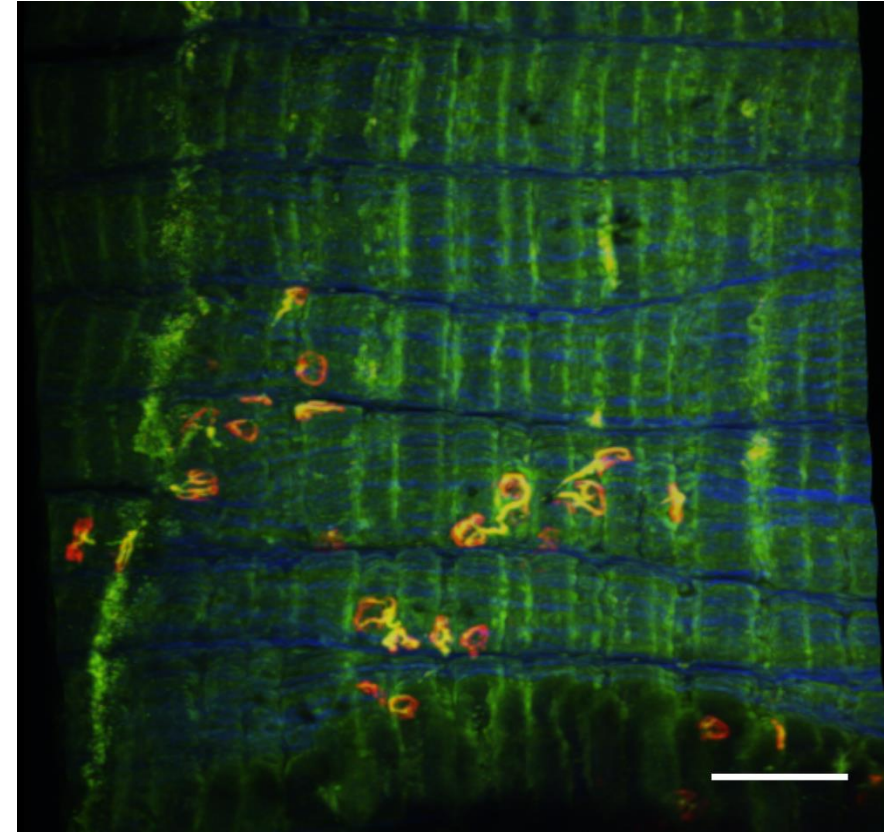
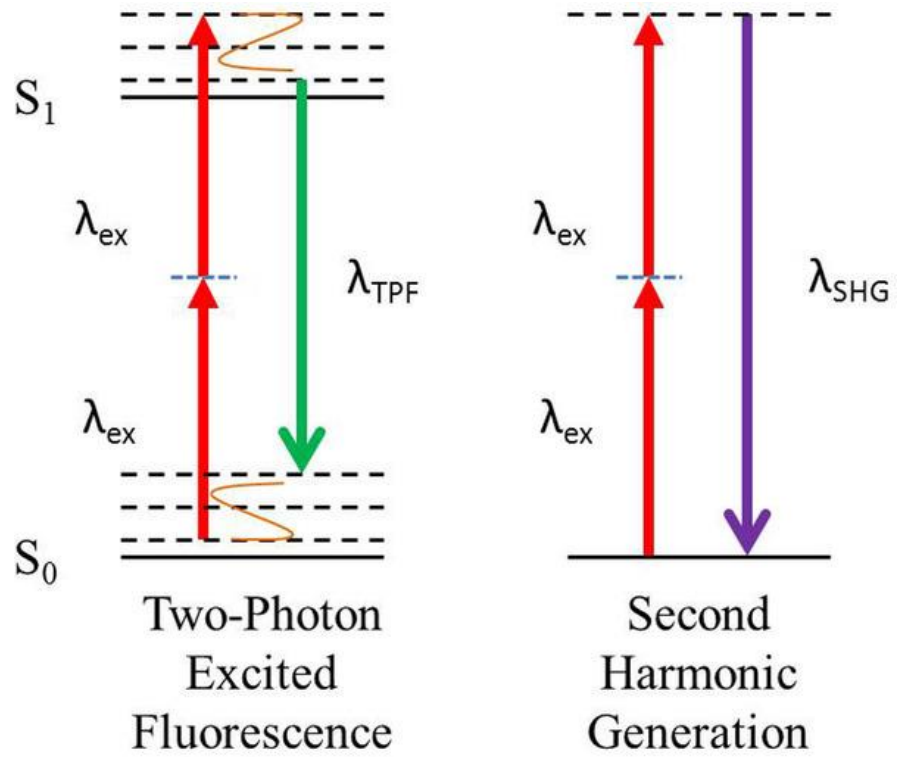


Figure 6



Two-photon Microscopy of Neuromuscular Junction Endplates  
Yu Cheung / Richard Webster / Susan Maxwell / Prof. David Beeson



Scale Bar = 100  $\mu\text{m}$

Neurofilament (Green) / Bungarotoxin/AChR (Red) / Second Harmonic Generation (Blue)

## Zeiss Cell Observer Spinning Disc Confocal



- The Zeiss Cell Observer spinning disc confocal has been optimized for high-speed, high-sensitivity, time-lapse CONFOCAL imaging of live cells at 37C and 5% CO<sub>2</sub>.
- This system is equipped with lasers (405, 458, 488, 514, 561, and 633 nm) , CCD cameras, and emission filters for imaging in the visible spectrum

# Spinning Disk Confocal

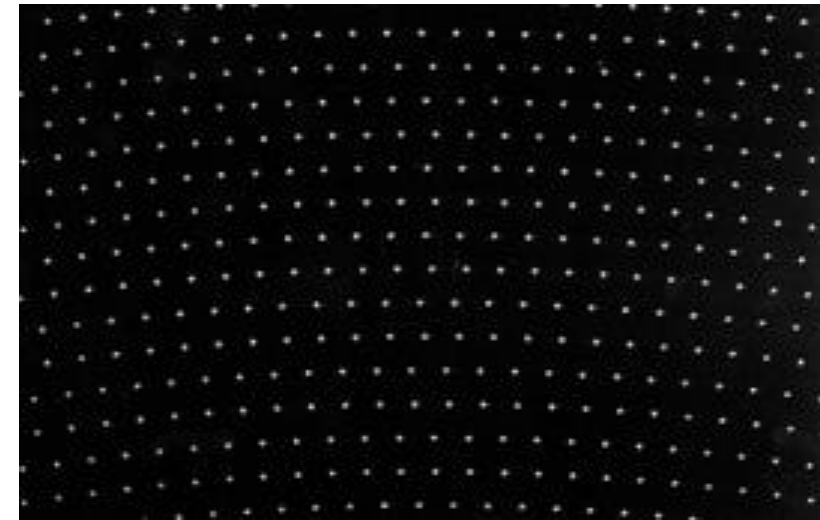
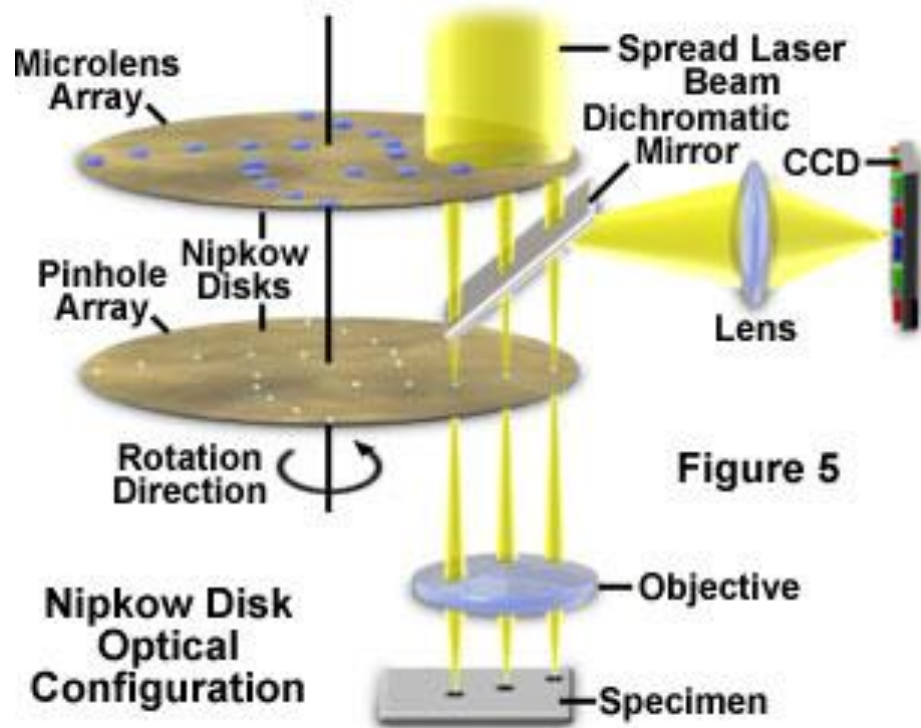
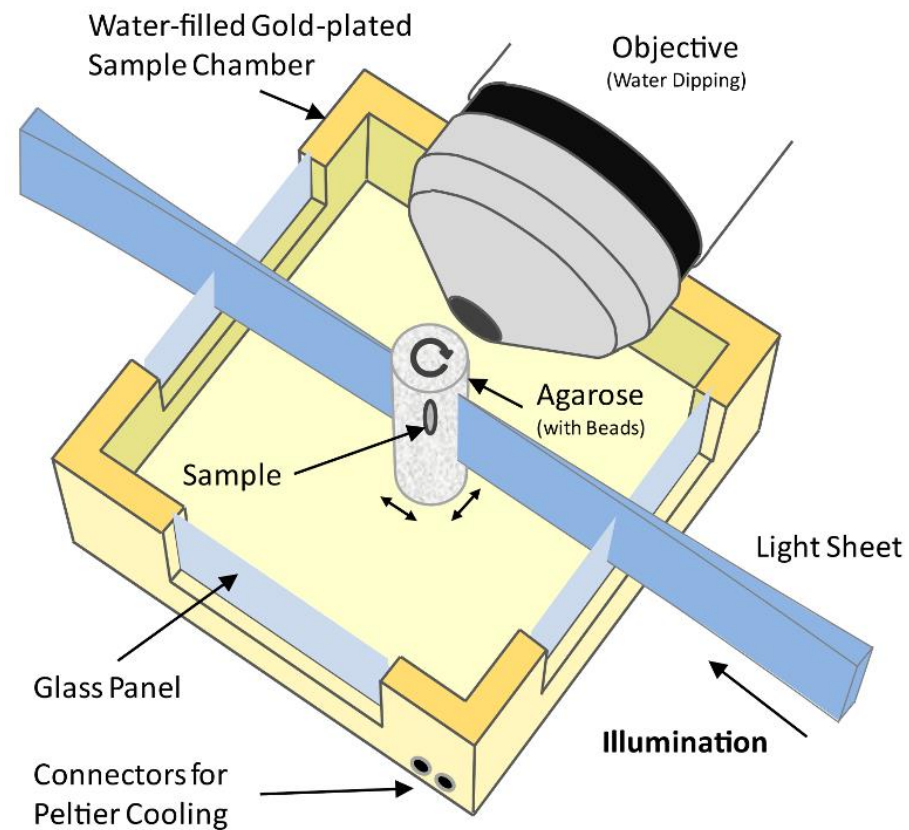


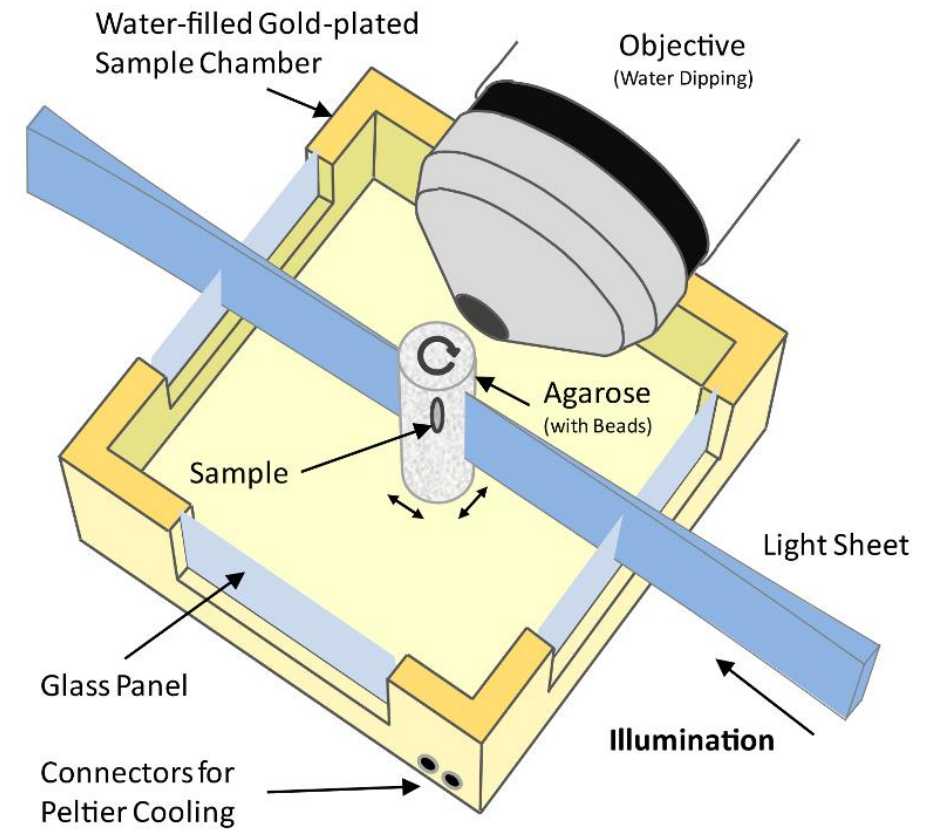
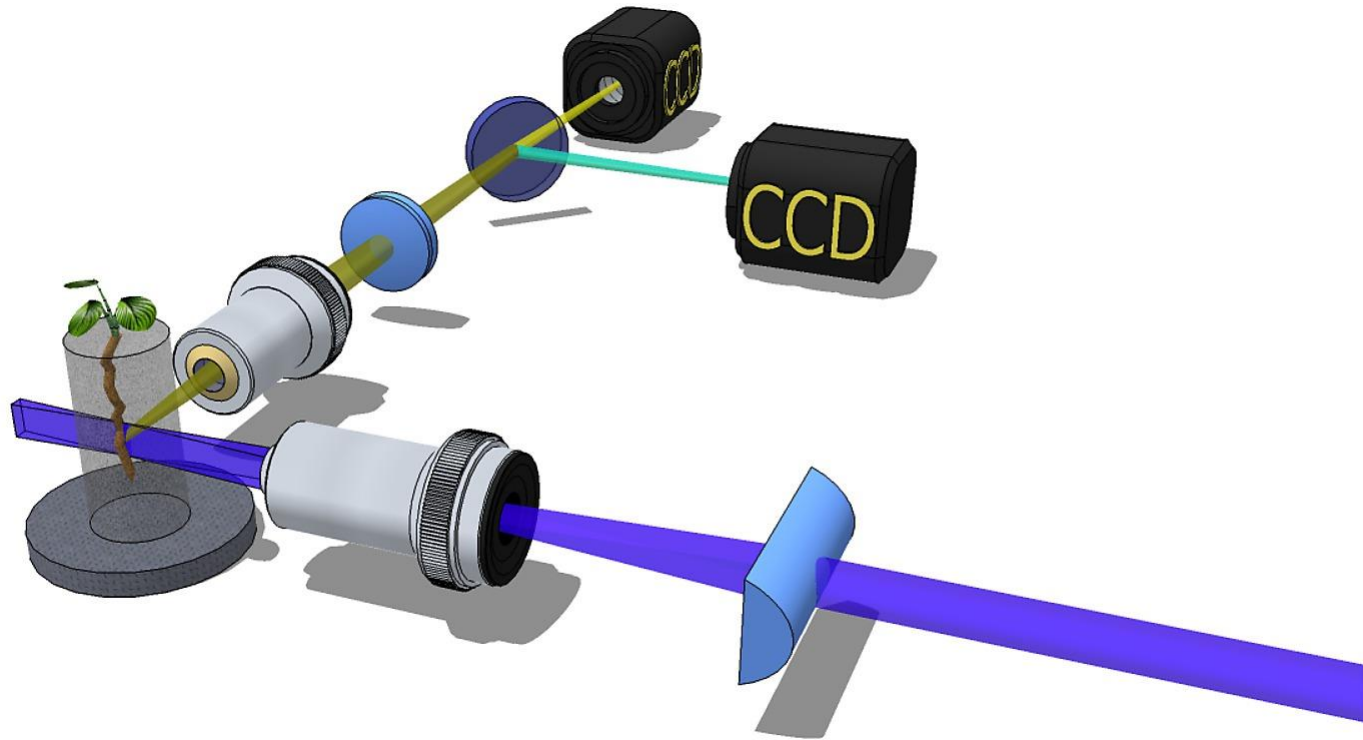
Image with many pinholes at once, so fast

Use CCD as detector, so much higher QE

# Zeiss Z1 Light Sheet Microscope

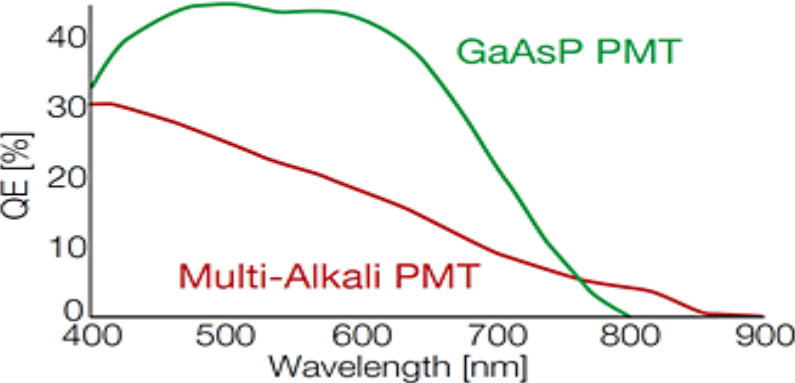


# Light sheet microscope

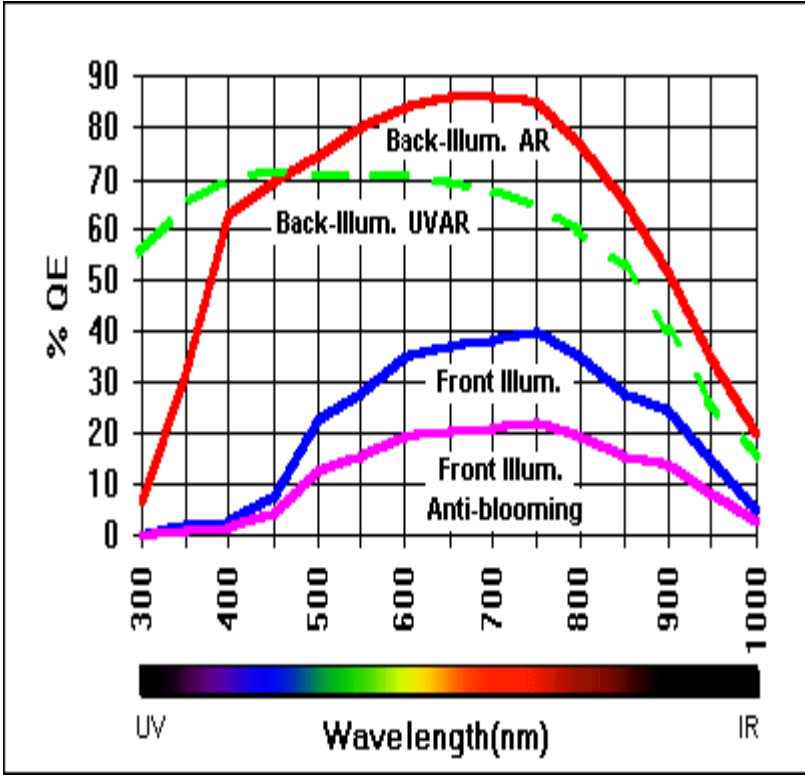


# Detectors - PMTs vs CCDs

Standard Quantum Efficiencies of Detector Technologies



Laser scanning confocals  
Multi-photon confocals



Wide-field microscopes  
Spinning-disc confocals  
Light sheet microscopes



## Comparison of Widefield/Deconvolution and Confocal Microscopy for Three-Dimensional Imaging

Peter J. Shaw

### INTRODUCTION

The biggest limitation inherent in optical microscopy is its lateral spatial resolution, which is determined by the wavelength of the light used and the numerical aperture (NA) of the objective lens. Another important limitation is the resolution in the direction of the optical axis, conventionally called  $z$ , which is related to the depth of field. The presence of a finite aperture gives rise to undesirable and rather complicated characteristics in the image. In essence, the depth of field depends on the size of structure or spatial frequency being imaged. Fine image detail, which is generally of most interest, has a small depth of field, and only features within a small distance of the focal plane contribute to the image. On the other hand, large structures — low spatial frequency components — have a relatively large depth of field, and contribute to the detected image seen at distant focal planes. This is very noticeable in dark-field imaging modes, such as epi-fluorescence, and means that the fine image detail may be swamped by low resolution “out-of-focus” light and thus either lost, or visualized with very much reduced contrast.

The principle advantage of confocal microscopy for biological imaging is that the optical arrangement has the effect of eliminating much of the out-of-focus light from detection, therefore improving the fidelity of focal sectioning (and hence the three-dimensional imaging properties), and increasing the contrast of the fine image detail. But the rejection of the out-of-focus light necessarily means that a proportion of the light emitted by the specimen is intentionally excluded from measurement. All illumination of the specimen has deleterious effects — bleaching of the fluorochrome or phototoxicity to living cells. These specimen-dependent factors are the ultimate limitation to the quality of the image, and inevitably confocal imaging does not detect much of the emitted light.

An alternative way of removing the out-of-focus light involves recording images at a series of focal planes using a conventional microscope, often called widefield (WF) to distinguish it from confocal imaging, and then using a detailed knowledge of the imaging process to correct for it by computer image processing. This procedure is called deconvolution, and its application to biological problems actually preceded the widespread introduction of biological confocal microscopes (Castleman, 1979; Agard and Sedat, 1983; Agard *et al.*, 1989). In contrast to confocal imaging, up to 30% of the total fluorescent light emitted by the specimen can be recorded (i.e., all the light that can be collected by a single, high-NA objective). This chapter examines the question: Is it better to record all the light emitted and process the WF images to

redistribute the out-of-focus light to produce a more accurate three-dimensional (3D) image, or to exclude the out-of-focus light from measurement in the first place by confocal optics and then deconvolve the confocal data?

### THE POINT SPREAD FUNCTION: IMAGING AS A CONVOLUTION

In order to derive a soundly based description of the degradation introduced by an optical microscope, especially if any attempt is to be made to reverse this degradation, it is necessary to be able to describe the relation between the specimen and its optical image in mathematical terms. We shall give here a very condensed explanation — the interested reader is referred elsewhere for more rigorous mathematical derivations (Agard *et al.*, 1989; Shaw, 1993; Young, 1989; and Chapters 20, 21, 22, 24, and 25, *this volume*). Within some quite general limitations, the object (specimen) and image are related by an operation known as convolution. In a convolution, each point of the object is replaced by a blurred image of the point having a relative brightness proportional to that of the object point. The final image is the sum of all these blurred point images. The way each individual point is blurred is described by the point spread function (PSF), which is simply the image of a single point. This is illustrated diagrammatically in Figure 23.1.

The conditions that must be met for an imaging process to be described as a convolution are that it should be linear and shift invariant (Young, 1989). Imagine cutting the specimen into two parts and imaging each part separately with the microscope. If adding these two subimages together produces the same result as imaging the whole specimen, and does this irrespective of how the specimen is cut up, then the imaging is said to be linear. If the imaging is indeed linear, then the specimen can be imagined cut up into smaller and smaller pieces, until the size of each piece is well below the resolution limit, and can be considered to be simply a point. The image is then the sum of the images of each of the points, each multiplied by a function corresponding to the amount of light coming from that point. The multiplication and summing is represented mathematically by an operation called convolution. Shift invariance simply means that the imaging characteristics and thus the PSF are the same over the whole field of view, and knowing one PSF is enough to characterize the imaging properties of the microscope. (Agard *et al.*, 1989; Shaw and Rawlins, 1991a).

Although imaging modes such as phase contrast and differential interference contrast (DIC) are not linear, because their contrast depends on differences of refractive index within the object,

TABLE 23.1. Summary of Pros and Cons of 3D Microscopy Methods

	Wide-Field Deconvolution	Single Spot Confocal	Scanning-Disk Confocal	Two-Photon
Effective detector QE.	60%–80% (CCD)	3%–12% (PMT)	60%–80% (CCD)	3%–12% (PMT)
Detector noise (rms $\sigma$ /pixel)	4–12	<1	4–12 (<1 for EM-CCD)	<1
Peak signal (photons/pixel)	>30,000	20–100	~5000	20–100
Acquisition time (s/frame)	Depends on CCD readout (>0.05)	0.2–10	Depends on CCD readout (>0.05)	0.2–10
Peak excitation intensity/ $\mu\text{m}^2$	10 nW	1 mW	1 $\mu\text{W}$	10 W
Excitation wavelengths	Hg arc 350–650 nm	Available laser lines	Available laser lines	Ti:Sa 700–900 nm

# Light-sheet fluorescence microscopy for quantitative biology

Ernst H K Stelzer

In light sheet–based fluorescence microscopy (LSFM), optical sectioning in the excitation process minimizes fluorophore bleaching and phototoxic effects. Because biological specimens survive long-term three-dimensional imaging at high spatiotemporal resolution, LSFM has become the tool of choice in developmental biology.

Although transmitted light microscopy provides a view of the morphology of a specimen, the ability to tag specific organs, organelles or macromolecules with fluorophores allows one to localize well-defined subsets of targets in the specimen. Fluorescence microscopy images have high contrast, showing bright targets on a dark background.

In conventional wide-field and confocal epifluorescence microscopes, the same lens is used for the excitation of the fluorophore and the collection of the emitted fluorescence. The excitation light passes through the specimen and, assuming uniform fluorophore distribution, excites the same number of fluorophores in each focal plane along its optical axis. Therefore, whenever an epifluorescence microscope focuses on a plane along its optical axis, it actually excites all the fluorophores in a specimen, including those above and below the focal plane.

The optical sectioning capability of a confocal fluorescence microscope is based on discrimination against the out-of-focus fluorescence light by a pinhole in an image plane in front of the intensity detector. The excitation of a fluorophore and the detection of a fluorescence photon are independent events. Although the excitation intensity is conserved along the optical axis, the fluorescence emission intensity, which is

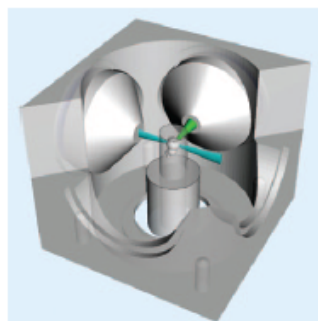


**Figure 1** | Basic optical arrangement in LSFM. In contrast to an epifluorescence arrangement, LSFM uses at least two independently operated lenses. The lenses used for fluorophore excitation are arranged at a 90° angle relative to those used for detection. Only a thin planar section in the specimen centered on the focal planes of the detection lenses is illuminated. The specimen is maintained in a close-to-natural 3D state.

proportional to the square of the excitation intensity, is not; it actually has a maximum in the focal plane. Only optical instruments whose fluorescence intensity detection depends on the product of two independent events have this property of optical sectioning and thus an axial resolution<sup>1,2</sup>. In other words, wide-field fluorescence microscopes have no axial resolution.

To make matters worse, fluorescence microscopy has several basic limitations. First, the excitation light is absorbed not only by fluorophores but also by many endogenous organic compounds, which

are degraded much like fluorophores<sup>3</sup> and thus are unavailable for vital metabolic processes. Second, the number of fluorophores in any volume element at any given time is finite, and fluorophores can degrade upon excitation. As a consequence, the number of photons that can be retrieved from a fluorophore-labeled specimen is limited. Finally, life on Earth is adapted to the solar flux, which is less than 1.4 kW/m<sup>2</sup>. This might not be a hard limit, but it indicates that irradiance should not exceed 1 nW/μm<sup>2</sup> = 100 mW/cm<sup>2</sup> when dynamic biological processes are observed (Box 1).

*In toto*, as long as we rely on epifluorescence microscopes, we are faced with two serious challenges. First, both fluorophores and specimens are essentially wasted during the observation process; second, all fluorophores and many endogenous organic compounds in the specimen are excited whenever we record a single plane. Obviously, the situation becomes even more challenging when we perform complex biological experiments and observe the behavior of multiple targets in three dimensions as a function of time.

For imaging living biological samples, these challenges must be addressed. LSFM<sup>4</sup> is perhaps the best technique we have so far with which to make a sincere and honest effort: it provides optical sectioning and a true axial resolution, reduces fluorophore bleaching and phototoxicity at almost any scale, allows one to record millions of pixels in parallel and dramatically improves the viability of the specimen (Table 1).

## BOX 1 PHOTOTOXICITY IN LIVE-SAMPLE IMAGING.

To how much light can one expose a biological specimen? There is no general answer, but all those who have worked with fluorescence and even transmission light microscopy are aware of the negative effects of illumination on the viability of a specimen. There are some general findings: (i) phototoxic effects are more obvious at lower rather than at higher wavelengths, (ii) the presence of fluorophores has a dramatic negative impact<sup>3</sup> and (iii) both low intensity and low energy of the illumination light are desirable. Assuming that many organic molecules will absorb the excitation light without fluorescing but will still degrade, it is probably safe to suggest that any imaging of live specimens should be performed at a level that avoids even moderate fluorophore bleaching.

A hint might be provided by the solar constant, which is around 1.4 kW/m<sup>2</sup> at the equator and around 1 kW/m<sup>2</sup> in central Europe. In microscopic terms, this is about 1 nW/μm<sup>2</sup> or 100 mW/cm<sup>2</sup>. Hence, one can calculate that the maximal radiant exposure should be around 0.5 μJ/μm<sup>2</sup> and infer that cells and small model embryos should not be exposed to more than a few millijoules and a few hundred millijoules, respectively. Very few microscopes can operate at these low levels, i.e., in the ‘single sun’ regime. The light sheet–based fluorescence microscope is one of them. Confocal fluorescence and super-resolution microscopes usually operate in a ‘multiple-suns’ regime. This may pose a substantial problem for live-specimen imaging.

Solar constant at equator	1,366 W/m <sup>2</sup> = 1,366 J/s · m <sup>2</sup>
Solar constant in central Europe	~ 1 kW/m <sup>2</sup>
Microscopy relevant units	~ 1 nW/μm <sup>2</sup> = 100 mW/cm <sup>2</sup>
Energy density within 600 s	~ 0.6 μJ/μm <sup>2</sup>
Cell diameter of 100 μm × (0.3 s or 10 min)	~ 2.4 μJ or 4.8 mJ
Embryo diameter of 900 μm × (0.3 s or 10 min)	~ 190 μJ or 380 mJ

Ernst H.K. Stelzer is at the Buchmann Institute for Molecular Life Sciences, Fachbereich Lebenswissenschaften (FB15, IZN), Goethe Universität Frankfurt am Main, Frankfurt am Main, Germany.  
e-mail: ernst.stelzer@physikalischebiologie.de

Article

## Light Dose is a Limiting Factor to Maintain Cell Viability in Fluorescence Microscopy and Single Molecule Detection

Michael Wagner <sup>1</sup>, Petra Weber <sup>1</sup>, Thomas Bruns <sup>1</sup>, Wolfgang S. L. Strauss <sup>2</sup>, Rainer Wittig <sup>2</sup> and Herbert Schneckenburger <sup>1,2,\*</sup>

<sup>1</sup> Institut für Angewandte Forschung, Hochschule Aalen, Beethovenstr. 1, D-73430 Aalen, Germany; E-Mails: michael.wagner@htw-aalen.de (M.W.); petra.weber@htw-aalen.de (P.W.); thomas.bruns@htw-aalen.de (T.B.)

<sup>2</sup> Institut für Lasertechnologien in der Medizin und Meßtechnik an der Universität Ulm, Helmholtzstr. 12, D-89081 Ulm, Germany; E-Mails: wolfgang.strauss@ilm.uni-ulm.de (W.S.L.S.); rainer.wittig@ilm.uni-ulm.de (R.W.)

\* Author to whom correspondence should be addressed; E-Mail: herbert.schneckenburger@htw-aalen.de; Tel.: +49-7361-576-3401.

Received: 14 January 2010; in revised form: 20 February 2010 / Accepted: 21 February 2010 /

Published: 8 March 2010

---

**Abstract:** A test system for cell viability based on colony formation has been established and applied to high resolution fluorescence microscopy and single molecule detection. Living cells were irradiated either by epi-illumination or by total internal reflection (TIR) of a laser beam, and light doses where at least 90% of irradiated cells survived were determined. These light doses were in the range of a few J/cm<sup>2</sup> up to about 200 J/cm<sup>2</sup> depending on the wavelength of illumination as well as on the presence or absence of a fluorescent dye (e.g., the membrane marker laurdan). In general, cells were less sensitive to TIR than to epi-illumination. However, comparably high light doses needed for repetitive excitation of single molecules limit the application of super-resolution microscopy to living cells.

**Keywords:** cell viability; light dose; fluorescence microscopy; TIR; single molecules

---

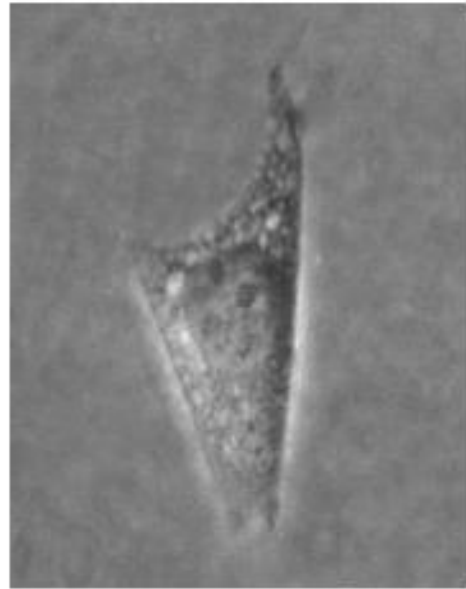
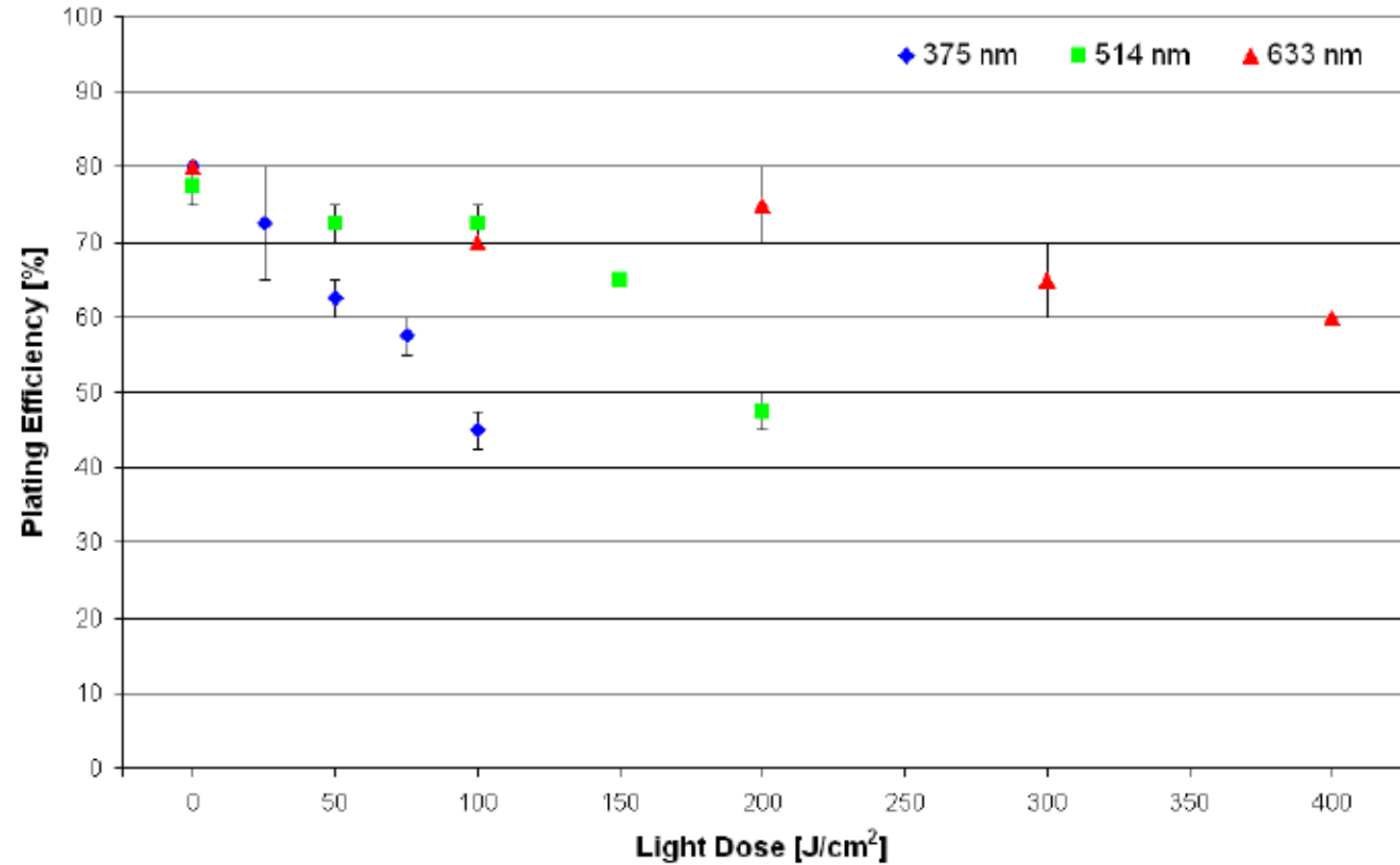
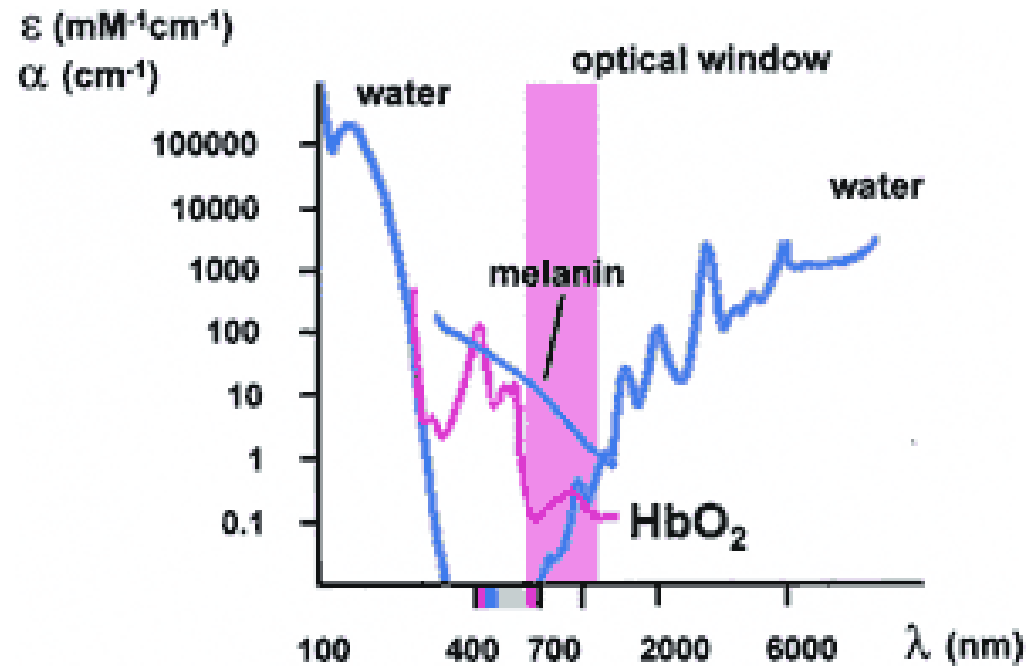


**Figure 3.** Percentage of colony formation (“plating efficiency”) of single non-incubated U373-MG glioblastoma cells upon exposure to different excitation wavelengths and light doses. Values represent medians  $\pm$  MADs. The plating efficiency at 0 J/cm<sup>2</sup> is defined as 100% cell survival.



## Two-photon Microscopy is superior for thick specimen



- Less susceptible to loss of signal due to scattering
- Low tissue absorption at 700-1000 nm

## Advances in multiphoton microscopy for imaging embryos

Willy Supatto<sup>1</sup>, Thai V Truong<sup>2</sup>, Delphine Débarre<sup>1</sup> and Emmanuel Beaurepaire<sup>1</sup>

Multiphoton imaging is a promising approach for addressing current issues in systems biology and high-content investigation of embryonic development. Recent advances in multiphoton microscopy, including light-sheet illumination, optimized laser scanning, adaptive and label-free strategies, open new opportunities for embryo imaging. However, the literature is often unclear about which microscopy technique is most adapted for achieving specific experimental goals. In this review, we describe and discuss the key concepts of imaging speed, imaging depth, photodamage, and nonlinear contrast mechanisms in the context of recent advances in live embryo imaging. We illustrate the potentials of these new imaging approaches with a selection of recent applications in developmental biology.

### Addresses

<sup>1</sup>Laboratory for Optics and Bioscience, Ecole Polytechnique ParisTech, CNRS, and INSERM U896, Palaiseau, France

<sup>2</sup>Biological Imaging Center, California Institute of Technology, Pasadena, CA, USA

Corresponding author: Supatto, Willy ([willy.supatto@polytechnique.edu](mailto:willy.supatto@polytechnique.edu))

Current Opinion in Genetics & Development 2011, 21:538-548

This review comes from a themed issue on Developmental mechanisms, patterning and evolution Edited by Sean Megason, Shankar Srinivas, Mary Dickinson and Anna-Katerina Hadjantonakis

Available online 13th September 2011

0959-437X/\$ – see front matter

© 2011 Elsevier Ltd. All rights reserved.

DOI 10.1016/j.gde.2011.08.003

### Introduction

From a microscopy perspective, live embryos present uniquely challenging characteristics compared to other biological samples. Embryos are smaller than 1 mm, at least during early developmental stages, making them accessible for three-dimensional (3D) imaging with light microscopy. However, they typically have an ellipsoidal shape and their inner structure is inhomogeneous and constantly changing. In addition, embryos are sensitive to manipulation and photodamage, and their labeling can be difficult. These properties challenge the performance of microscopy techniques in terms of imaging depth, imaging speed, photodamage and contrast. Since its introduction in 1990 [1], 2-photon excited fluorescence (2PEF) microscopy has proven to be the most effective approach for deep tissue fluorescence microscopy (Box 1).

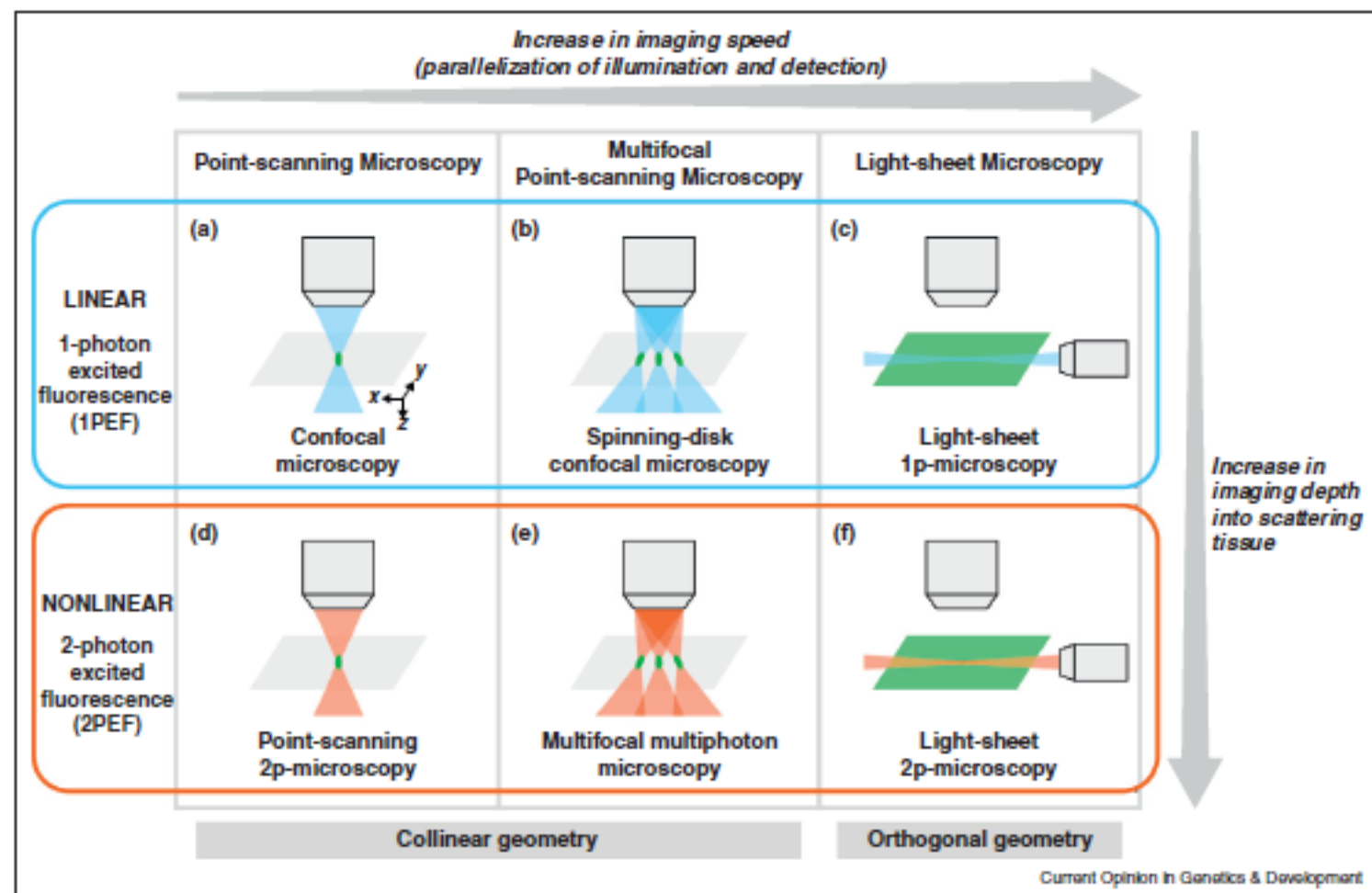
It has found many applications in neuroscience [2–3] and more recently in other fields, such as in immunology [4]. Multiphoton (or nonlinear) imaging is attractive also for embryo imaging and in recent years has been applied to an increasing number of published studies in developmental biology using various model systems, such as fruit fly [5–8], quail [9], zebrafish [10], or mouse embryos [11–12]. Multiphoton imaging is also promising for addressing current issues in systems biology and high-content experimental investigation of embryonic development [13] requiring novel methods for faster and deeper imaging of embryos with better contrast and resolution. In this review we analyze the parameters limiting imaging speed and depth in the currently available imaging modalities, and we discuss promising recent advances in multiphoton microscopy of live embryos, including light-sheet excitation and label-free imaging.

### Fast imaging of live embryos with multiphoton light-sheet microscopy

Imaging developmental processes often requires time-lapse 3D-image acquisitions (4D imaging). The imaging speed of a microscope can be defined by its pixel (or voxel) rate, that is, the number of pixels per unit time that can be obtained with sufficient signal and contrast. A high pixel rate permits capturing with adequate time resolution fast processes such as heart development (50–130 frames per second (fps) in Refs. [14,15,16\*\*]), cilia beating (900 fps in Ref. [17]) or fluid flow in developing embryos (44 fps in Ref. [18]). A high pixel rate is also required to study slower large-scale processes such as collective cell migration or cell division patterns with a large number of pixels per image to reach the appropriate spatial resolution: for instance, *in toto* imaging of early development [16\*\*,19–20] typically requires acquiring ~100 million voxels per 3D-image stack in less than a minute.

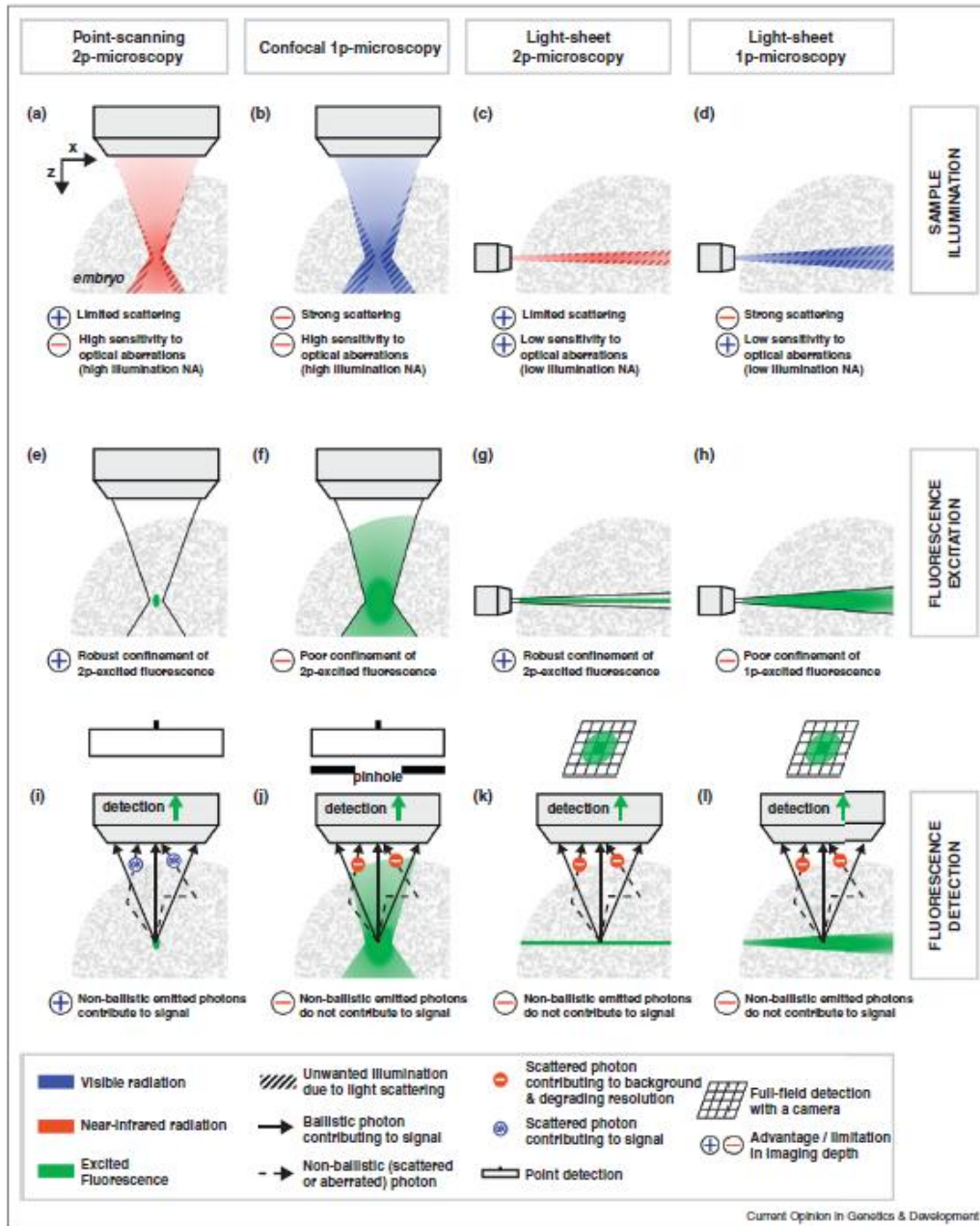
In this context, point-scanning confocal or multiphoton approaches are usually too slow, as the image is recorded one pixel at a time (Figure 1). Indeed, in these approaches signal level prescribes pixel accumulation times of typically 1–10  $\mu$ s, corresponding to pixel rates of only  $10^5$ – $10^6$  pixels  $s^{-1}$ .

Several approaches have been explored during the last 15 years to improve the imaging speed of multiphoton microscopy up to ~ $10^7$  pixels  $s^{-1}$ , including fast point-scanning and multifocal approaches (Figure 1, Tables 1 and 2, and [21] for a review). However, besides hardware limitations (i.e. scanning speed, readout time, data transfer or storage)



Strategies for improving acquisition speed in current fluorescence microscopy techniques. Similar strategies have been developed in linear (a–c) and nonlinear (d–f) microscopy. Both point-scanning (a and d) and multifocal (b and e) approaches use a collinear geometry: the illumination and the detection paths are collinear. Light-sheet microscopy (c and f) uses an orthogonal geometry: the illumination path is orthogonal to the detection path. Pixel rate range typically from  $10^5$ – $10^6$  pixels  $s^{-1}$  in point-scanning microscopy to  $10^7$ – $10^8$  pixels  $s^{-1}$  in light-sheet microscopy. While nonlinear microscopy in general provides deeper imaging than linear microscopy, differences exist in imaging depth performance between the different implementations of nonlinear microscopy, as discussed in the text.

Figure 3



# Quantitative high-speed imaging of entire developing embryos with simultaneous multiview light-sheet microscopy

Raju Tomer, Khaled Khairy, Fernando Amat & Philipp J Keller

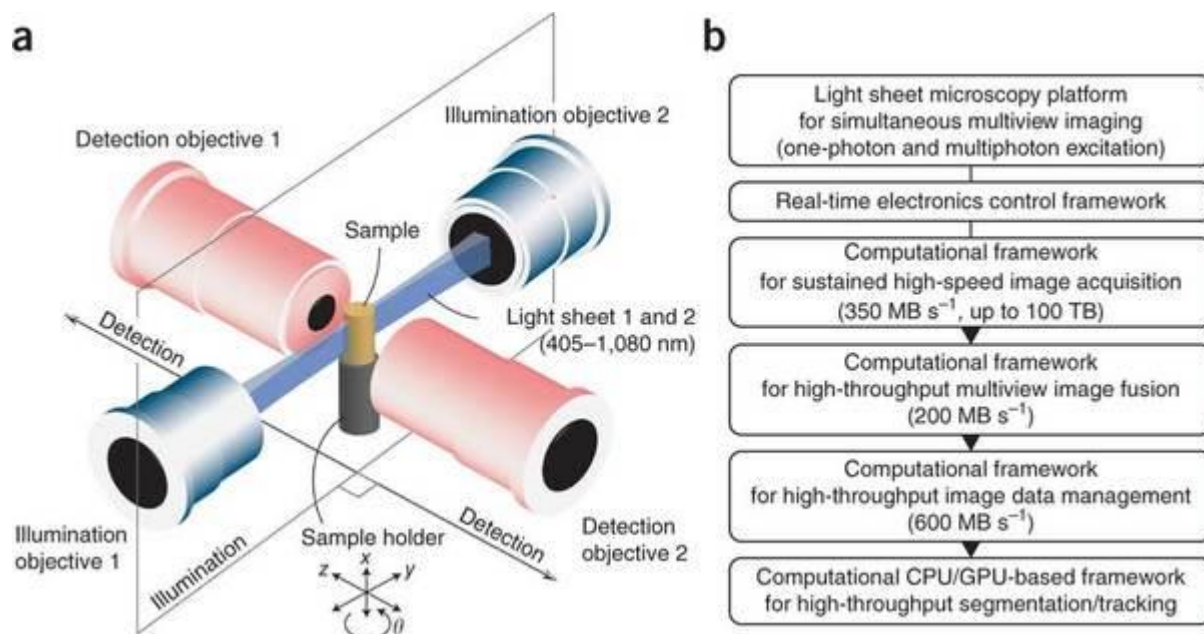
Live imaging of large biological specimens is fundamentally limited by the short optical penetration depth of light microscopes. To maximize physical coverage, we developed the SIMView technology framework for high-speed *in vivo* imaging, which records multiple views of the specimen simultaneously. SIMView consists of a light-sheet microscope with four synchronized optical arms, real-time electronics for long-term sCMOS-based image acquisition at 175 million voxels per second, and computational modules for high-throughput image registration, segmentation, tracking and real-time management of the terabytes of multiview data recorded per specimen. We developed one-photon and multiphoton SIMView implementations and recorded cellular dynamics in entire *Drosophila melanogaster* embryos with 30-s temporal resolution throughout development. We furthermore performed high-resolution long-term imaging of the developing nervous system and followed neuroblast cell lineages *in vivo*. SIMView data sets provide quantitative morphological information even for fast global processes and enable accurate automated cell tracking in the entire early embryo.

Understanding the development and function of complex biological systems relies on our ability to record and quantify fast spatiotemporal dynamics on a microscopic scale. Owing to the fundamental trade-off between spatial resolution, temporal resolution and photodamage, the practical approach in biological live imaging has been to reduce the observation of large systems to small functional subunits and to study these one at a time. Although this strategy has advanced our knowledge in past decades, holistic approaches are now required to visualize and analyze complex systems, such as developing embryos, in their entirety: the ability to resolve the spatiotemporal dynamics of biological processes on a systems level is indispensable for understanding the morphological development of complex tissues<sup>1,2</sup> and entire organisms<sup>3,4</sup>, the global analysis of gene expression patterns<sup>5,6</sup>, the systematic dissection of functional relationships in the developmental building plan<sup>7,8</sup>, and the implementation of high-throughput approaches to automated screening<sup>9</sup> and cellular phenotyping<sup>10</sup>.

Light-sheet microscopy techniques are evolving into essential tools for the *in vivo* study of biological structure and function at a systems level<sup>11–13</sup>. They are based on the simple yet effective idea of illuminating a specimen with a thin sheet of laser light and recording orthogonally the fluorescence emitted from this thin volume. Only the in-focus part of the specimen is exposed to laser light, which provides optical sectioning and substantially reduces photodamage. Moreover, the fluorescence signal emitted from the in-focus section is detected in parallel for the entire field of view, which provides high imaging speeds. In comparison to confocal microscopy, the most commonly used optical sectioning technique, light-sheet microscopy offers faster imaging, higher signal-to-noise ratio and lower photo-bleaching rates by up to several orders of magnitude<sup>14</sup>. Advances in the past few years have led to enhanced spatial<sup>15</sup> and temporal<sup>16</sup> resolution as well as breakthroughs in the conceptual design and complexity of live imaging experiments<sup>4</sup>.

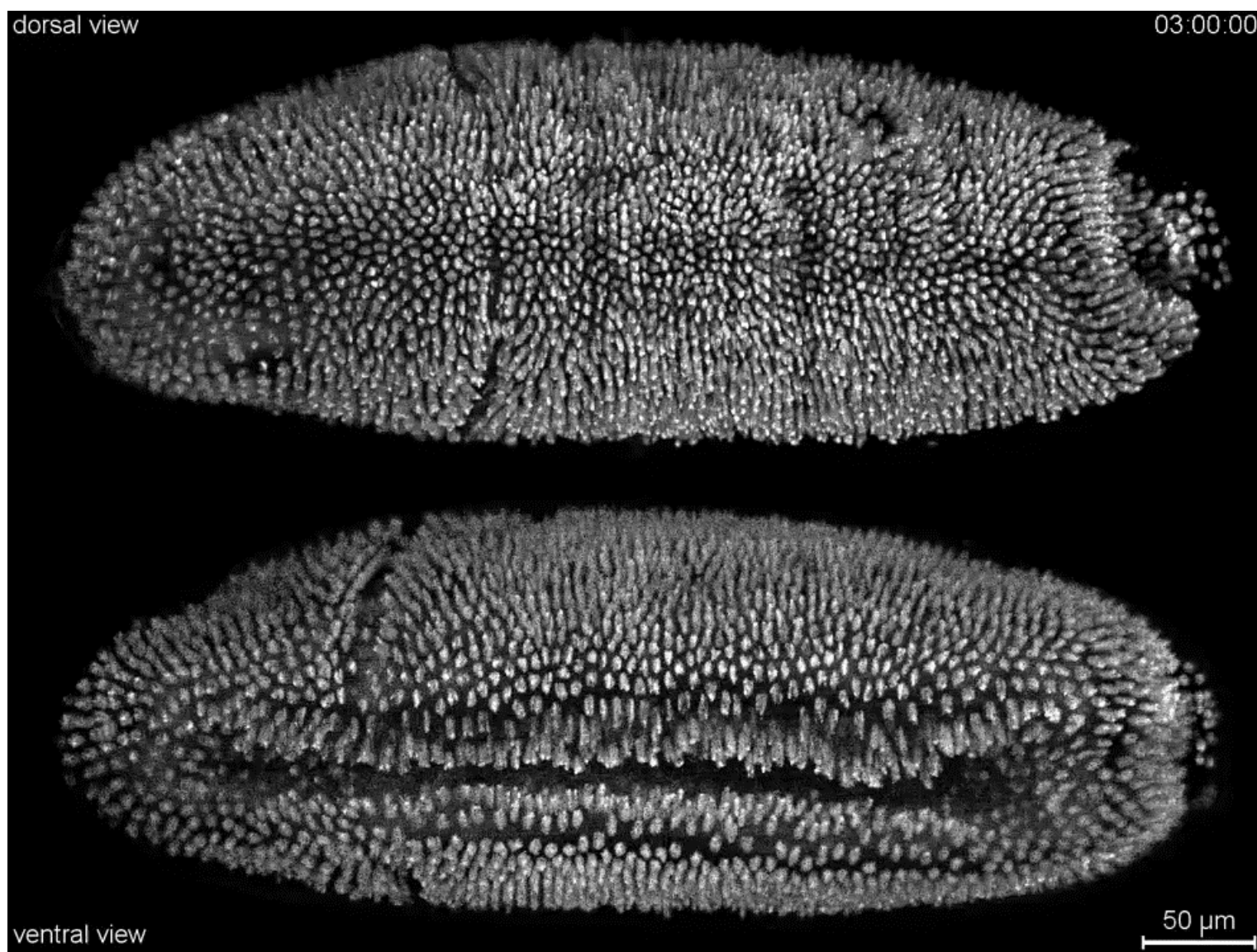
However, the optical penetration depth in light-sheet microscopes is fundamentally limited by light scattering: light microscopy in general does not penetrate more than several tens to hundreds of microns of living tissue, which precludes systems-level imaging in many biological model organisms<sup>17</sup>. Although penetration can be increased by nonlinear excitation<sup>15,18,19</sup>, this practical limitation persists because neither one-photon nor multiphoton light-sheet microscopes allow imaging of large multicellular organisms in their entirety from a single view<sup>3,19</sup>.

This limitation is partially overcome by sequential multiview imaging, in which the sample is rotated and image stacks are sequentially acquired from multiple view angles<sup>3,4,19,22</sup>. Sequential multiview imaging is generally suitable for fixed specimens, but it is inherently slow and thus fails to capture fast processes in live specimens. In live multicellular organisms, fast developmental processes can occur between the sequential multiview acquisitions and prevent accurate image fusion of the acquired data. The resulting spatiotemporal artifacts constrain quantitative analyses such as the reconstruction of cell tracks and cell morphologies. For global measurements of the dynamic behavior and structural changes of all cells in a developing organism, data



Howard Hughes Medical Institute, Janelia Farm Research Campus, Ashburn, Virginia, USA. Correspondence should be addressed to P.J.K. (kellerp@janelia.hhmi.org).

RECEIVED 28 SEPTEMBER 2011; ACCEPTED 20 APRIL 2012; PUBLISHED ONLINE 3 JUNE 2012; DOI:10.1038/NMETH.2062



Simultaneous multiview imaging of *Drosophila* embryonic development (*His2Av-GFP<sup>S65T</sup>* transgenic stock). The embryo was recorded at 30-second intervals over a period of 17 hours, using an image acquisition period of 15 seconds per time point. The data set consists of 1,066,520 high-resolution images (11 terabytes). The video shows separate maximum-intensity projections of the first and second halves of the fused and background-corrected three-dimensional image stacks, providing dorsal and ventral views of the developing embryo. To reduce the file size of this video, frames were down-sampled by a factor of 2. Imaging framework: One-photon SiMView. Detection objectives: 2× Nikon CFI75 LWD 16×/0.80 W. Cameras: 2× Andor Neo sCMOS. Technical note: The occurrence of subtle stripe patterns arises from column gain variability in first-generation sCMOS cameras, such as the Andor Neo cameras used in this recording.

20. T. Pizzari, C. K. Cornwallis, H. Lavie, S. Jakobsson, T. R. Birkhead, *Nature* **426**, 70 (2003).
21. M. Olsson, R. Shine, T. Madsen, A. Gullberg, H. Tegstam, *Nature* **383**, 585 (1996).
22. A. Puzosy, M. Wolf, *Trends Ecol. Evol.* **11**, 201 (1996).
23. T. Imogen, N. Wedell, *Nature* **415**, 71 (2002).
24. J. Merilä, L. E. B. Kruuk, B. C. Sheldon, *Nature* **412**, 76 (2001).
25. T. Venn *et al.*, *Nature* **411**, 45 (2001).
26. J. Merilä, B. C. Sheldon, S. C. Griffith, *Ann. Zool. Fenn.* **40**, 269 (2003).
27. W. G. Eberhard, *Female Control: Sexual Selection by Cryptic Female Choice* (Princeton Univ. Press, Princeton, NJ, 1996).
28. S. C. Griffith, *Am. Nat.* **169**, 274, discussion 282 (2007).
29. We thank T. Birkhead, R. Brooks, R. Calbeck, S. Immler, S. Ulstund, D. Westmat, and M. Whiting for comments on the manuscript. This work was supported by Discovery Grants DP0770889 (S.R.P.) and DP0881019 (S.C.G.) from the Australian Research Council, a UDeaf for Women in Science Fellowship (S.R.P.), and the Save the Goulfish

Fund. The Animal Care and Ethics Committee of Macquarie University approved this research.

**Supporting Online Material**  
www.sciencemag.org/cgi/content/full/329/5994/964/DC1  
Materials and Methods  
Fig. S1  
Table S1  
References  
17 May 2010; accepted 7 July 2010  
10.1126/science.1192407

## Cell Lineage Reconstruction of Early Zebrafish Embryos Using Label-Free Nonlinear Microscopy

Nicolas Olivier,<sup>1\*</sup> Miguel A. Luengo-Oroz,<sup>2\*</sup> Louise Duloquin,<sup>3\*</sup> Emmanuel Faure,<sup>4</sup> Thierry Savy,<sup>4</sup> Israël Veilleux,<sup>1</sup> Xavier Solinas,<sup>1</sup> Delphine Dèbère,<sup>1</sup> Paul Bourging,<sup>4,5</sup> Andrés Santos,<sup>2</sup> Nadine Peyrieras,<sup>3,6,†</sup> Emmanuel Beaurepaire<sup>1,†</sup>

Quantifying cell behaviors in animal early embryogenesis remains a challenging issue requiring in toto imaging and automated image analysis. We designed a framework for imaging and reconstructing unstained whole zebrafish embryos for their first 10 cell division cycles and report measurements along the cell lineage with micrometer spatial resolution and minute temporal accuracy. Point-scanning multiphoton excitation optimized to preferentially probe the innermost regions of the embryo provided intrinsic signals highlighting all mitotic spindles and cell boundaries. Automated image analysis revealed the phenomenology of cell proliferation. Blastomeres continuously drift out of synchrony. After the 32-cell stage, the cell cycle lengthsens according to cell radial position, leading to apparent division waves. Progressive amplification of this process is the rule, contrasting with classical descriptions of abrupt changes in the system dynamics.

Although classical developmental biology is characterized by qualitative descriptions, recent work underlines the requirements for precise measurements to enable formal reconstruction integrating the genetic, molecular, and cellular levels of organization (1–3). The optimization of microscopy imaging techniques and improved data algorithmic processing are key issues in such reconstructions. Parallelized linear microscopy such as light-sheet fluorescence microscopy provides fast imaging but suffers from loss of information with depth (4). Point-scanning two-photon microscopy provides deeper imaging (5) but exhibits slower frame rate, compromising

automated individual cell tracking in whole organisms (6). Furthermore, the usual implementation of these two paradigms does not allow homogeneous illumination in spherical samples, leading to a difficult tradeoff between the detection of deep structures and illumination-induced perturbation in outer layers. Finally, relying on fluorescent staining of biological structures brings additional artifacts and limitations. Exploiting the intrinsic optical nonlinear properties of the sample is a valuable, although challenging, alternative. Second-harmonic generation (SHG) is obtained from dense noncentrosymmetric structures such as oriented microtubule assemblies (7–9), including mitotic spindles (8, 10). Third-harmonic generation (THG) is obtained from optical heterogeneities (11)—such as the interface between an aqueous medium and a lipidic, mineralized, or absorbing structure (12)—and allows morphological imaging of small organisms (10, 13).

Here, we show that combining SHG and THG imaging of unlabeled embryos with a scanning scheme matching embryo morphology provides adequate three-dimensional (3D) imaging over time for the automated reconstruction of cell behavior during zebrafish embryo cleavage stages (14). Ad hoc image analysis strategies for cell position, division, and shape identification were used to produce a complete and validated lineage

tree for a cohort of six zebrafish embryos until the 1000-cell stage, annotated with minute-level division timing, micrometer-accuracy cell coordinates, and shape characteristics. These data provided a quantitative spatiotemporal description of the wave-like division cycles and allowed the construction of a prototypic digital blastula. The cycle duration of sister cells exhibited variability that did not correlate with cell volume, revealing unexpected cell division asynchrony and asymmetry from the first division cycles and leading to increasing cell heterogeneity by the time of midblastula transition (MBT) (14).

An appropriate image acquisition scheme was devised to provide high-resolution time-lapse imaging of intrinsic SHG and THG signals (Fig. 1 and supporting online material). Excitation in the 1.2- $\mu\text{m}$  range reduced nonlinear endogenous absorption by the sample and allowed simultaneous two-photon-excited fluorescence (2PEF) imaging of red fluorescent proteins (Fig. 1, B and C) for control experiments. When imaging a spherical embryo, scattering and aberrations typically result in reduced signal at the center of each plane (Fig. 1E). We therefore scanned each plane of a half-sphere along a spiral trajectory with variable speed to spend more time imaging the innermost cells (Fig. 1, D to F, and fig. S1). This conformal strategy provided optimal acquisition time and minimal photoperturbation (fig. S2). SHG and THG signals were co-optimized by using rotating linear incident polarization. In addition, because THG contrast from a specific structure depends on its size relative to the focal volume (15), moderate focusing (3.5- $\mu\text{m}$  Z-resolution) was used to highlight cell interface compared with smaller subcellular structures (Fig. 2D).

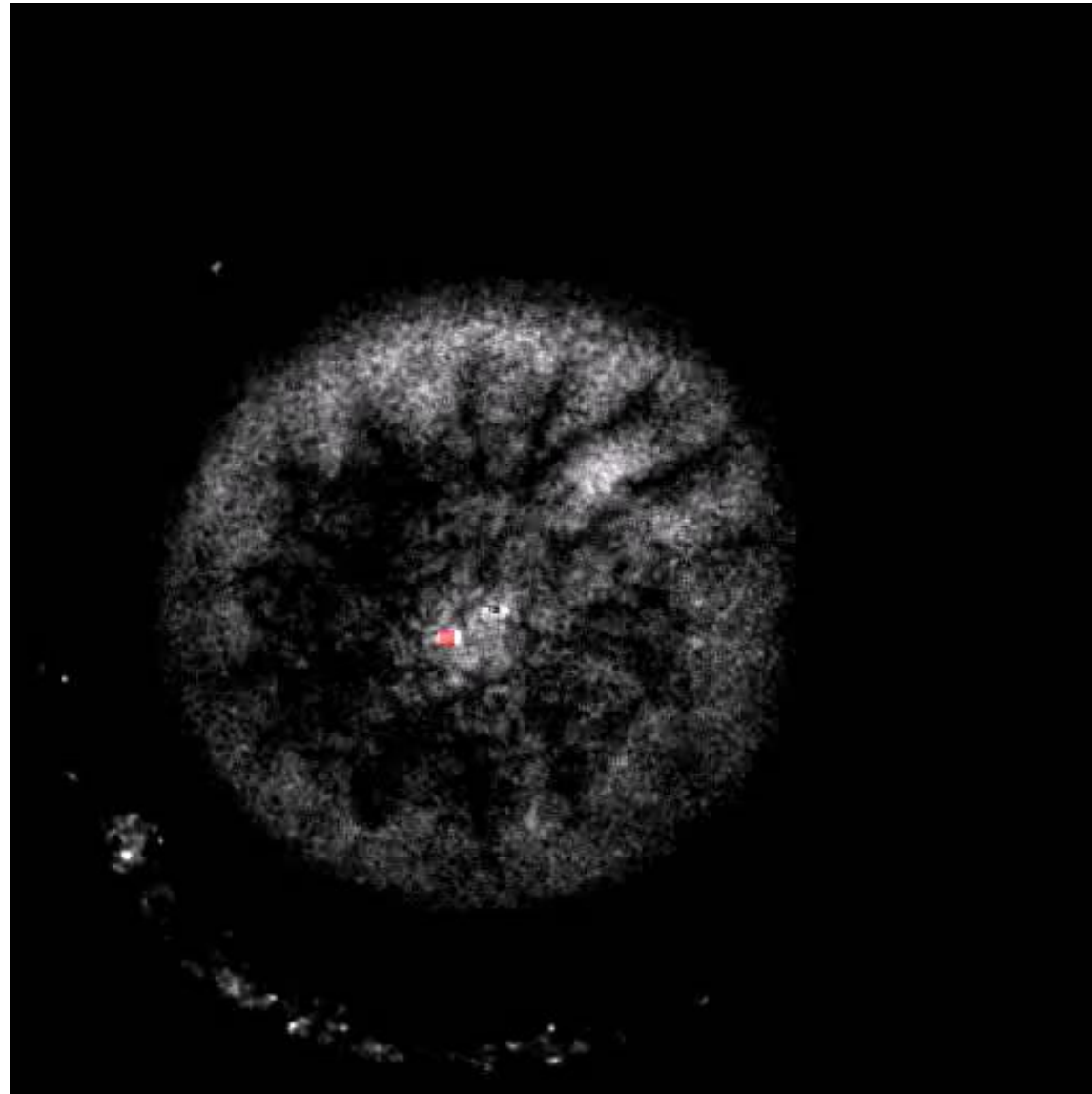
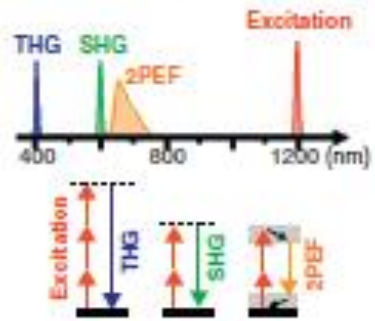
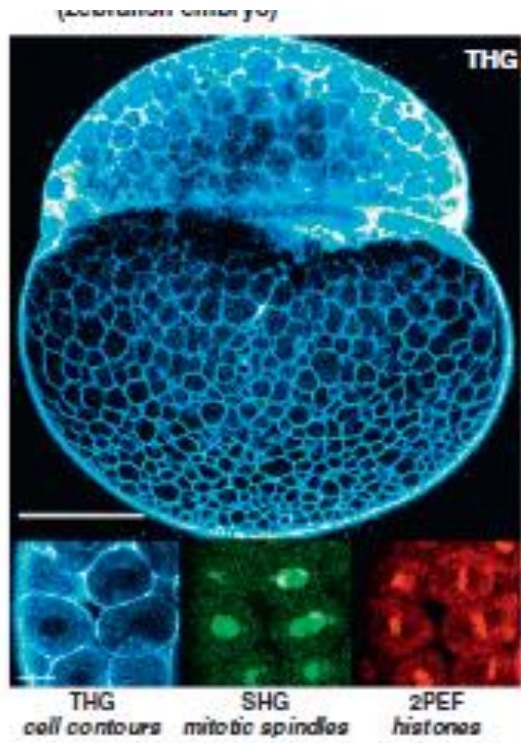
Combining the conformal scanning scheme described above, sensitive detection, infrared excitation wavelength, and appropriate focusing and polarization conditions allowed homogenous detection of mitotic spindles and cell and tissue phenotypic features in the whole unlabeled zebrafish embryo during cleavage stages. The blastoderm was contained in a half sphere of 440- $\mu\text{m}$  radius imaged with a temporal resolution of 80 s and a volumetric pixel size of 2 by 2 by 4  $\mu\text{m}$ , suitable for further automated reconstruction of the cell lineage tree.

The intrinsic THG signal revealed a number of structures and dynamic processes (Fig. 2, A to J, and movies S1 to S6) and highlighted cell contours even better than membrane staining by

<sup>1</sup>Laboratory for Optics and Biosciences, Ecole Polytechnique, CNRS, INSERM, Palaiseau, France. <sup>2</sup>Biomedical Image Technologies, Universidad Politécnica de Madrid, and Biomedical Research Center in Bioengineering, Biomaterials, and Nanomedicine (CIBER-BBN), Madrid, Spain. <sup>3</sup>Neurobiologie et Développement, Institut de Neurobiologie Alfred Fessard, CNRS, Gif/Yvette, France. <sup>4</sup>Centre de Recherche en Epithémiologie Appliquée, Ecole Polytechnique, CNRS, Paris, France. <sup>5</sup>Réseau National des Systèmes Complexes, 57-59 rue Lhomond, Paris, France. <sup>6</sup>Institut des Systèmes Complexes Paris Ile-de-France, 57-59 rue Lhomond, Paris, France.

\*These authors contributed equally to this work.

†To whom correspondence should be addressed. E-mail: nadine.peyrieras@inra.fr (N.P.); emmanuel.beaurepaire@polytechnique.edu (E.B.)



Algorithmic detection of mitotic spindles from SHG images

# Other Practical Considerations

- Temperature
- pH (Phenol Red)
- Humidity
- Auto-fluorescence (NADH, FAD, ...)
- Photo-toxicity
- Coverslip thickness (# 1 ½)
- Non-invasive labeling

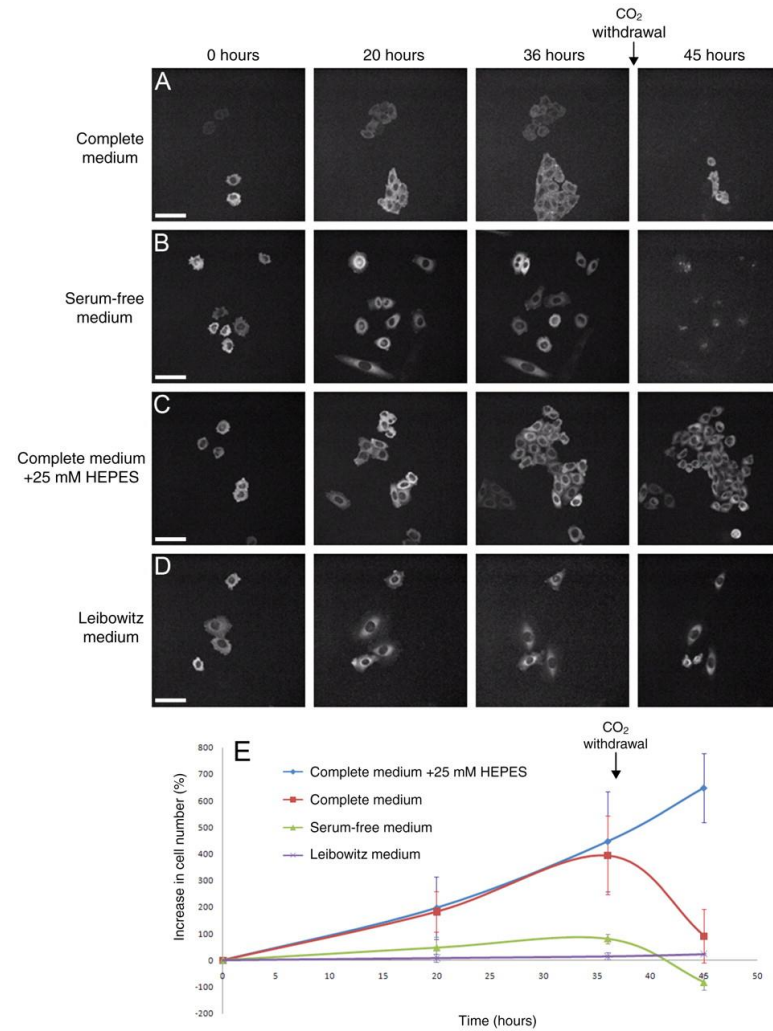
# Environmental Variables for Mammalian Cell Lines

Variable	Optimum Range	Comments
Temperature	28-37°C	Control with Specimen Chamber Heaters Use Inline Perfusion Heaters Objective Lens Heaters Environmental Control Boxes
Oxygenation	Variable	Perfuse or Change Media Regularly Use Large Chamber Volume
Humidity	97-100 Percent	Closed (Sealed) Chamber Humidified Environmental Chamber Auto-Fill System for Open Chambers
pH	7.0-7.7	Use HEPES Buffered Media Perfuse or Change Media Regularly No Phenol Red Indicator
Osmolarity	260-320 mosM	Avoid Evaporation Closed (Sealed) Chamber Humidified Environmental Chamber
Atmosphere	Air or 5-7 Percent Carbon Dioxide	Use HEPES Buffered Media for Air Closed (Sealed) Chamber Atmosphere Controlled Chamber
Media Buffer	Bicarbonate or Synthetic Biological Buffers	Beware of Phototoxicity Closed and Open Chambers Atmosphere Controlled Chamber

# Temperature and CO<sub>2</sub> Control



# Effects of the type of medium and the presence or absence of CO<sub>2</sub> on cell proliferation.



Frigault M M et al. J Cell Sci 2009;122:753-767

## Phenol Red free media



Opti-MEM® I Reduced-Serum Medium is an improved Minimal Essential Medium (MEM) that allows for a reduction of [Fetal Bovine Serum](#) supplementation by at least 50% with no change in cell growth rate or morphology. Opti-MEM® I medium is also recommended for use with cationic lipid transfection reagents, such as Lipofectamine™ reagent. Opti-MEM® I medium can be used with a variety of suspension and adherent mammalian cells, including Sp2, AE-1, CHO, BHK-21, HEK, and primary fibroblasts.

# Live Cell Imaging Buffer

A recipe for a HEPES buffered imaging medium (Brown et al. 2000 Traffic 1:124-140)

Imaging Medium Stock (5x) pH 7.4

750 mM NaCl

100 mM HEPES

5 mM CaCl<sub>2</sub>

25 mM KCl

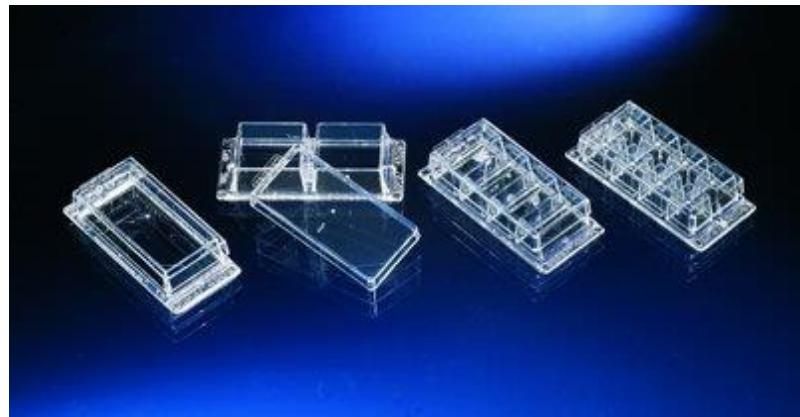
5 mM MgCl<sub>2</sub>

Use at 1x. On day of use add 95 mg glucose and 95 mg albumin to 50 ml of medium. Warm to 37°C. Keep cells in incubator in their usual medium until immediately before imaging. When ready to image, remove their usual medium and replace it with imaging medium.

Cells can normally be kept on the stage in this medium for 30-60 min.



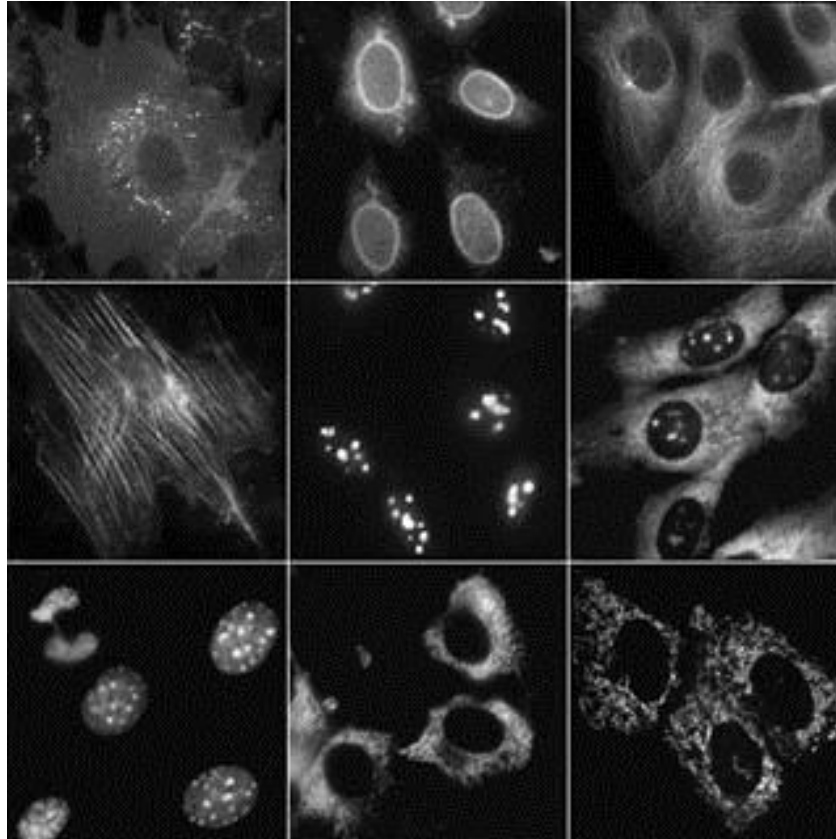
35mm Glass Bottom Culture Dish



Nunc™ Lab-Tek™ Chambered Coverglass



# EGFP-Fusion proteins



Jarvik JW, Fisher GW, Shi C, Hennen L, Hauser C, Adler S, Berget PB.  
In vivo functional proteomics: Mammalian genome annotation using CD-tagging.  
BioTechniques 2002; 33: 852-866.